iScience

CellPress

Article

# Pib2-Dependent Feedback Control of the TORC1 Signaling Network by the Npr1 Kinase

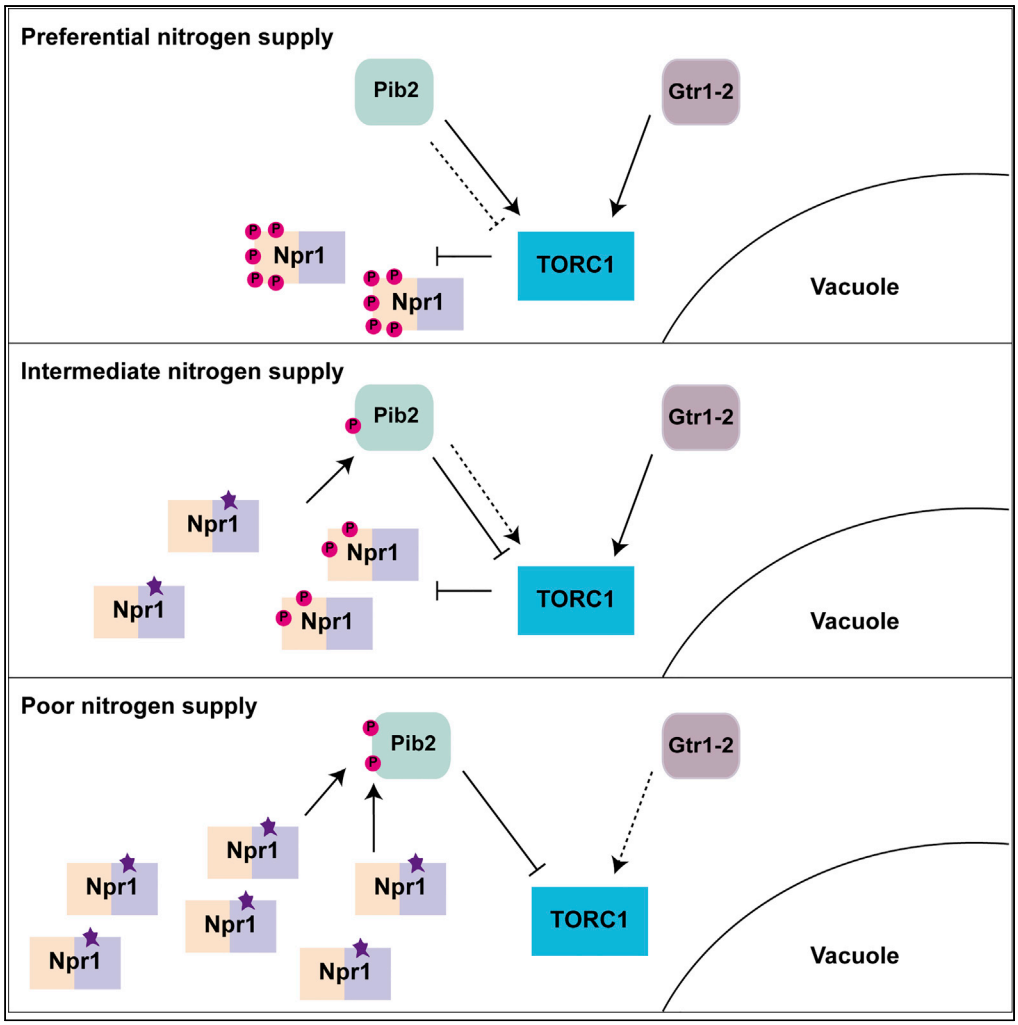


Ana Sofia Brito, Silvia Soto Diaz, Pascale Van Vooren, Patrice Godard, Anna Maria Marini, Mélanie Boeckstaens

mboeckst@ulb.ac.be

## HIGHLIGHTS

pH drop linked to nitrogen entry is correlated with TORC1 phosphorylation of Npr1

Cytosolic acidification is not a prerequisite for TORC1 activation

Gtr1/Gtr2 and Pib2 both independently regulate Npr1 phosphorylation and activity

Npr1 mediates a Pib2-dependent inhibition of TORC1

Brito et al., iScience *20*, 415–433
October 25, 2019 
https://doi.org/10.1016/j.isci.2019.09.025

iScience

CellPress

Article

# Pib2-Dependent Feedback Control of the TORC1 Signaling Network by the Npr1 Kinase

Ana Sofia Brito,[1,3] Silvia Soto Diaz,[1,3] Pascale Van Vooren,[1,3] Patrice Godard,[2] Anna Maria Marini,[1] and Mélanie Boeckstaens[1,4,*]

## SUMMARY

**To adjust cell growth and metabolism according to environmental conditions, the conserved TORC1 signaling network controls autophagy, protein synthesis, and turnover. Here, we dissected the signals controlling phosphorylation and activity of the TORC1-effector kinase Npr1, involved in tuning the plasma membrane permeability to nitrogen sources. By evaluating a role of pH as a signal, we show that, although a transient cytosolic acidification accompanies nitrogen source entry and is correlated to a rapid TORC1-dependent phosphorylation of Npr1, a pH drop is not a prerequisite for TORC1 activation. We show that the Gtr1/Gtr2 and Pib2 regulators of TORC1 both independently and differently contribute to regulate Npr1 phosphorylation and activity. Finally, our data reveal that Npr1 mediates nitrogen-dependent phosphorylation of Pib2, as well as a Pib2-dependent inhibition of TORC1. This work highlights a feedback control loop likely enabling efficient downregulation and faster re-activation of TORC1 in response to a novel stimulating signal.**

## INTRODUCTION

Tuning of metabolic flux and development of survival responses are key processes for all cells to cope with variation of environmental conditions, notably in terms of nutrient availability or stressful surroundings. These adaptations rely on efficient sensing and signal transduction pathways that regulate transcriptional, translational, and post-translational aspects. In response to nutrient availability and growth factors in metazoans, the target of rapamycin (TOR) signaling network plays a central role in all eukaryotes in the control of growth by regulating autophagy and protein synthesis and turnover (De Virgilio and Loewith, 2006; Eltschinger and Loewith, 2016; González and Hall, 2017; Howell et al., 2013; Loewith and Hall, 2011; Shimobayashi and Hall, 2014; Wullschleger et al., 2006). In line with its prevalent role in cell growth, alteration of mammalian mTOR signaling is associated with several disorders including obesity, diabetes, and cancer. Studies in the yeast model organism played an important role in the discovery of the Tor kinases and in the characterization of their functions. In yeast, Tor1 and Tor2 kinases are part of two conserved and structurally distinct multi-protein complexes named TORC1 (containing Tor1 or Tor2) and TORC2 (containing Tor2), only TORC1 being highly sensitive to rapamycin-mediated inhibition (Eltschinger and Loewith, 2016; Heitman et al., 1991; Loewith et al., 2002).

Under global nutrient sufficiency, yeast TORC1 is semi-uniformly associated with the membrane of the vacuole, the mammalian lysosome equivalent (Hughes Hallett et al., 2015; Kira et al., 2014; Prouteau et al., 2017; Varlakhanova et al., 2017). In these preferential growth conditions, TORC1 activates the Sch9 kinase signaling branch and stimulates the anabolic processes, leading to ribosome and protein synthesis, whereas it represses the Tap42-PP2A phosphatase branch required for the activation of environmental stress response, amino acid synthesis, nitrogen assimilation pathways, and the catabolic process of autophagy (Beck and Hall, 1999; Di Como and Arndt, 1996; Hughes Hallett et al., 2014; Prouteau et al., 2017; Urban et al., 2007). A recent study reports that spatially distinct pools of TORC1, localized at the surface of the vacuole or of the endosomes, control microautophagy, macroautophagy, and protein synthesis (Hatakeyama et al., 2019). Withdrawal of glucose, the major carbon and energy source, triggers an acute loss of TORC1 activity associated with downregulation of both Sch9 and Tap42-PP2A branches (Hughes Hallett et al., 2014; Urban et al., 2007). Hughes Hallet and coworkers propose that this glucose-starvation TORC1 inhibition is mediated by the AMP-activated protein kinase Snf1 (Hughes Hallett et al., 2014). Glucose starvation also leads to the redistribution of TORC1 to a single cylindrical structure of inactive

[1]Laboratory of Biology of Membrane Transport, IBMM, Université Libre de Bruxelles, rue des Professeurs Jeener et Brachet 12, 6041 Gosselies, Belgium

[2]UCB Pharma, Chemin du Foriest, 1420 Braine-l'Alleud, Belgium

[3]These authors contributed equally

[4]Lead Contact

*Correspondence: mboeckst@ulb.ac.be

https://doi.org/10.1016/j.isci.2019.09.025

oligomerized state, called TOROID, still associated with the vacuolar membrane (Prouteau et al., 2017). Nitrogen starvation, or rapamycin treatment, triggers a transition state in TORC1 activity, which downregulates the Sch9 branch and activates the Tap42-PP2A branch and the associated responses coping with nitrogen limitation (Hughes Hallett et al., 2014). Cytosolic pH ($pH_c$) is proposed to act as a signal activating TORC1 specifically in response to carbon availability (Dechant et al., 2014). The latter study discards a role of $pH_c$ in TORC1 activation in response to nitrogen availability, whereas others propose that $H^+$ influx coupled to nitrogen uptake could activate TORC1 (Dechant et al., 2014; Saliba et al., 2018).

TORC1 clearly plays an important role in nitrogen and amino acid responses, as deduced from deprivation and re-supplementation studies of a given amino acid in a corresponding auxotrophic strain (Binda et al., 2009; Yuan et al., 2017). Several mediators of the nitrogen and amino acid signal to TORC1 have been identified, although the global regulation scheme remains incomplete. At the vacuolar membrane, the EGO complex, made of a scaffold subcomplex of Ego proteins and the conserved Rag GTPases Gtr1 and Gtr2, stimulates TORC1 activity specifically when the heterodimeric Gtr1-Gtr2 subcomplex is composed of GTP-bound Gtr1 and GDP-bound Gtr2 (Binda et al., 2009; Gong et al., 2011; Kira et al., 2014; Nicastro et al., 2017). Pib2 is also involved in conveying a nitrogen signal to TORC1 and appears able to positively and negatively modulate the TORC1 activity (Kim and Cunningham, 2015; Michel et al., 2017; Tanigawa and Maeda, 2017; Varlakhanova et al., 2017). It remains controversial whether Pib2 acts independently of, or together with, the EGO complex. Moreover, upon deprivation of specific amino acids in a corresponding auxotrophic strain for which growth is sustained thanks to another abundant nitrogen source, the Gcn2 kinase downregulates TORC1 activity (Yuan et al., 2017). However, Gcn2 does not seem to play a role in response to the deprivation of the major nitrogen source that is supporting growth in conditions in which auxotrophies are complemented by small quantities of concerned amino acids. In addition to reacting to complete nitrogen starvation and single essential amino acid in auxotrophic strains, growth rate and TORC1 activity are modulated by the quality and the quantity of the nitrogen source (Godard et al., 2007; Stracka et al., 2014). It is noteworthy that the response to nitrogen availability varies according to the considered *Saccharomyces cerevisiae* genetic background, ammonium behaving as a preferential nitrogen source specifically in the Σ1278b background (Courchesne and Magasanik, 1983; Grenson, 1983a). The underlying mechanism and the involvement of TORC1 in the different nitrogen responses in relation to the strain background have not been deeply addressed.

In non-preferential nitrogen conditions, the Tap42-PP2A branch of TORC1 is stimulated (Hughes Hallett et al., 2014). One key effector of this branch is the Npr1 kinase, responding to nitrogen availability to regulate permeases of nitrogen compounds (Boeckstaens et al., 2007, 2014; 2015; Feller et al., 2006; Gander et al., 2008; Merhi and André, 2012; Neklesa and Davis, 2009; Schmidt et al., 1998). Npr1 fine-tunes the inherent activity of ammonium transport proteins by mediating the S457-phosphorylation and thereby inactivating the Mep2 auto-inhibitory domain and by controlling the phosphorylation of the intermediate Mep1 and Mep3 inhibitory partner, Amu1/Par32 (Boeckstaens et al., 2007, 2014; 2015). Npr1 further controls the stability of amino acid permeases (MacGurn et al., 2011; Merhi and André, 2012; Schmidt et al., 1998). In preferential nitrogen conditions, active TORC1 downregulates the Tap42-PP2A phosphatase branch and Npr1, which appears more phosphorylated, leading to inactivation or degradation of permeases. Direct interactions between TORC1 subunits and Npr1 suggest that the signaling complex directly phosphorylates the effector kinase (Breitkreutz et al., 2010). The phosphorylation status and activity of Npr1 are also proposed to be controlled by TORC1 via the Sit4 phosphatase, Npr1 being hyperphosphorylated and presumed inactive in the absence of the phosphatase (Jacinto et al., 2001). However, Npr1 is still able to positively regulate Mep2 in cells lacking the Sit4 phosphatase, indicating that activation of the Tap42-PP2A branch is not essential for Npr1 activity (Boeckstaens et al., 2014).

Here, we dissect the regulation of the Npr1 kinase by TORC1 using the Σ1278b genetic background in which ammonium behaves as a preferential nitrogen source. We study the signals required to inactivate Npr1, notably by evaluating a role of pH variation as a global signal controlling TORC1 in response to nitrogen availability. We show that, whatever the quality of the nitrogen source, the uptake of nitrogenous compounds is accompanied by a transient drop of cytosolic pH and a stimulation of Npr1 phosphorylation. However, our data highlight that cytosolic acidification is not a prerequisite for TORC1 activation. We show that the Gtr1 and Gtr2 GTPases and the Pib2 protein both regulate the TORC1-dependent phosphorylation and activity of Npr1 independently and in different ways. Our data further indicate that the N-terminal

regulatory and the C-terminal catalytic domains of the bipartite Npr1 kinase are involved in distinct functions. Finally, our results reveal that Npr1 participates in feedback control of TORC1 by downregulating the pathway via Pib2.

## RESULTS

### Nitrogen Source Entry Is Correlated to a Rapid and Transient Cytosolic Acidification

The phosphorylation status and activity of Npr1 are under the control of the TORC1 network that responds to nitrogen supply (Boeckstaens et al., 2014, 2015; Gander et al., 2008; Merhi and André, 2012; Neklesa and Davis, 2009; Schmidt et al., 1998). $pH_c$ has been proposed to act as a signal to activate TORC1 in response to carbon source availability (Dechant et al., 2014; Orij et al., 2012). More recently, $H^+$ influx associated with nitrogen source transport has also been proposed to activate TORC1 (Saliba et al., 2018). However, the related study failed to detect cytosolic acidification upon amino acid addition. We first addressed what could be the consequences on Npr1 global phosphorylation status of adding nitrogen sources of different quality to cells exponentially growing on proline minimal medium and further followed *in vivo* $pH_c$ variations upon nitrogen addition, using pHluorin. Addition of preferential nitrogen sources (glutamine, ammonium), intermediate-quality nitrogen source (glutamate), or non-preferential nitrogen sources (proline, citrulline, and valine) all triggered a rapid increase in Npr1 phosphorylation, suggesting a concomitant activation of TORC1 (Figure 1A). Npr1 phosphorylation was strongly inhibited in cells pre-treated with the TORC1-inhibitor rapamycin, demonstrating that this phosphorylation is TORC1 dependent. Except for proline addition to the initial proline-based medium, amino acid addition and, to a lesser extent, ammonium supplementation, all triggered a rapid transient drop in $pH_c$ (Figure 1B). The extent of the drop was not specifically associated with the quality of the nitrogen source, i.e., there was no correlation between the $pH_c$ variation and the added nitrogen source expected to lead to a modification of the growth rate (Godard et al., 2007). Glutamate triggered a larger and prolonged $pH_c$ drop. Ammonium triggered a limited $pH_c$ drop, whereas citrulline, valine, and glutamine triggered intermediate $pH_c$ drops. The apparent extent of Npr1 phosphorylation did not strictly reflect the extent of the cytosolic acidification (Figures 1A and 1B), suggesting that, if a decrease in $pH_c$ is transduced into a TORC1-activating signal, it is not the unique signal reporting the variation in nitrogen availability.

### Cytosolic Acidification Is Not a Prerequisite for TORC1 Activation

We next tested an alternative way to induce cytosolic acidification by using acetic acid addition and checked the consequences on the Npr1 phosphorylation pattern. Addition of acetic acid induced a rapid cytosolic acidification with a drop in $pH_c$ equivalent to that induced by glutamine (Figure 1B). However, acetic acid triggered a slight decrease in the detectable phosphorylation of Npr1 (Figure 1A), bolstering an absence of correlation between cytosolic acidification and the detectable phosphorylation pattern of the TORC1-effector Npr1. Hence, despite inducing a similar pH drop to the one observed with glutamine addition, the $pH_c$ decrease associated with acetic acid supplementation is not correlated with a TORC1 activation.

We further tested the impact of cytosolic acidification resulting from shifting cells grown in proline minimal medium buffered at initial pH 6.1 to a similar medium buffered at pH 2.3. Shifting cells to pH 2.3 buffered medium resulted in a transient drop of $pH_c$ equivalent to those observed after valine, citrulline, or glutamine addition, whereas shifting cells to a fresh medium buffered at pH 6.1, taken as control, resulted in an increase of $pH_c$ (Figure 1C). Despite the opposite modifications of $pH_c$, shifting cells to pH 2.3 or pH 6.1 medium both resulted in a similar rapid but transient Npr1 phosphorylation (Figure 1D), suggesting that the shift *per se*, and not the acidification, is responsible for this modification of the Npr1 phosphorylation profile. We also monitored the phosphorylation of another TORC1 target, an effector of the S6 branch, Rps6 (González et al., 2015). The pH shift induced a phosphorylation of Rps6 that was even more pronounced after shifting cells at pH 6.1 compared with pH 2.3, thus a condition in which a cytosolic basification is rather observed (Figures 1C and 1E).

We next addressed whether cytosolic acidification occurring upon nitrogen source entry could be a prerequisite for TORC1 activation. The preferred nitrogen source ammonium, known to stimulate TORC1 and cell growth, is transported by the specific ammonium transport proteins of the conserved Mep-Amt-Rh family (Marini et al., 1997). Cells deprived of the three *MEP* genes (triple-*mep4*) are unable to grow in the presence of ammonium concentrations below 5 mM (pH 6.1), whereas providing higher ammonium concentrations enables growth, likely due to a sufficient passive diffusion of the neutral

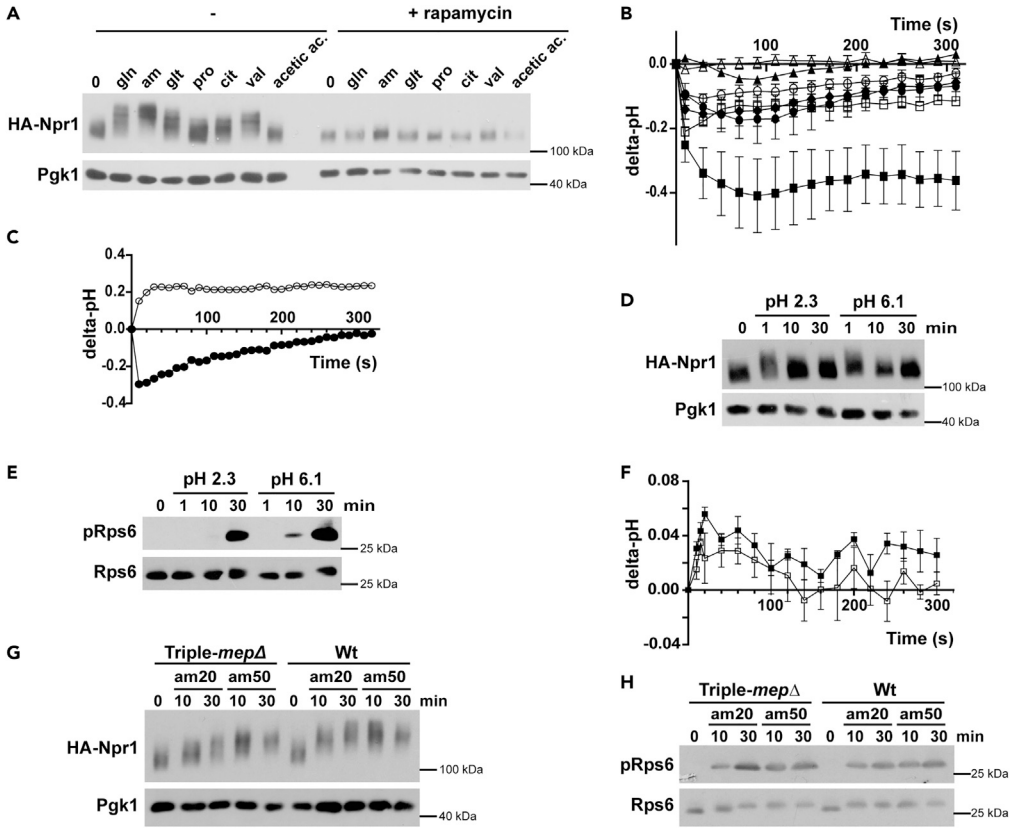


**Figure 1. Cytosolic Acidification, Associated with Nitrogen Source Entry, Is Not a Prerequisite for TORC1 Activation**

(A) Immunodetection of HA-Npr1 from total cellular extracts. Rapamycin (2 μg/mL) or the rapamycin vehicle alone (-, ethanol/tween) was added to the culture of proline-grown *npr1Δ* (30788a) cells transformed with the plasmid pAS103. One hour later ($t_0$), 10 mM glutamine (gln), ammonium (am), glutamate (glt), proline (pro), citrulline (cit), valine (val), or acetic acid was added during 5 min to the cell cultures. Pgk1 was detected as a loading control.

(B) Evolution of $pH_c$ corrected for negative control variations (delta-pH) after addition of 10 mM acetic acid (□), glutamine (●), ammonium (▲), glutamate (■), proline (Δ), citrulline (◆), or valine (○). Data are represented as mean ± SEM (n = 2 or 3). Wild-type (23344c) cells transformed with pYES-pHluorin were grown in the presence of proline as a nitrogen source.

(C–E) Cells were grown in a medium buffered at initial pH 6.1 and containing proline as the nitrogen source. At time t = 0, cells were collected by filtration and transferred to a similar medium buffered at pH 2.3 or 6.1. (C) Evolution of $pH_c$ after medium transfer (●, pH 2.3; ○, pH 6.1) of wild-type (23344c) cells transformed with pYES-pHluorin. (D) Immunodetection of HA-Npr1 from total extracts of wild-type (23344c) cells transformed with the plasmid pAS103. Pgk1 was detected as a loading control. (E) Immunodetection of pRps6 from total extracts of wild-type (23344c) cells transformed with pFL38. Total Rps6 was detected as a loading control.

(F) Evolution of $pH_c$ corrected for negative control variations (delta-pH) after addition of ammonium 20 (□) or 50 (■) mM. Data are represented as mean ± SEM (n = 3). Triple-*mepΔ* (31019b) cells were transformed with pYES-pHluorin and grown in the presence of proline as nitrogen source.

(G) Immunodetection of HA-Npr1 from total extracts of proline-grown triple-*mepΔ* (31019b) and wild-type (23344c) cells transformed with pAS103. Pgk1 was detected as a loading control.

(H) Immunodetection of pRps6 from total extracts of proline-grown triple-*mepΔ* (31019b) and wild-type (23344c) cells transformed with pFL38. Total Rps6 was detected as a loading control.

form $NH_3$. Accordingly, ammonium (20 or 50 mM) addition to triple-*mepΔ* cells induced at least a transient $pH_c$ increase (Figure 1F). Of note, ammonium addition to triple-*mepΔ* cells triggered the phosphorylation of Npr1 and of Rsp6, revealing that cytosolic acidification is not required for TORC1 activation occurring upon ammonium supplementation (Figures 1G and 1H).

Together, these results indicate that cytosolic acidification is not a prerequisite for TORC1 activation.

### Npr1 Phosphorylation and Activity Are Controlled by Snf1

We next dissected the contribution of known regulators of TORC1 to the phosphorylation and also to the activity of the Npr1 effector in the Σ1278b genetic background with one unique auxotrophy for uracil being complemented by an *URA3*-based plasmid. In response to different growth-related signals, such as nutrient availability, the activity of the central TORC1 complex is modulated by several regulators including the Gtr1 and Gtr2 GTPases, the Pib2 phosphatidylinositol 3-phosphate (PI3P) binding protein, and the Snf1 and Gcn2 kinases (Hughes Hallett et al., 2014; Kim and Cunningham, 2015; Nicastro et al., 2017; Yuan et al., 2017).

Of note, glucose withdrawal is known to be accompanied by cytosolic acidification, whereas TORC1 is inactivated, leading to a rapid dephosphorylation of Sch9 (Hughes Hallett et al., 2014; Orij et al., 2012; Prouteau et al., 2017; Urban et al., 2007). We evaluated the impact of glucose withdrawal on both Npr1 phosphorylation status and activity. Shifting proline-grown cells to a similar medium deprived of glucose was accompanied by an apparent two-phase change in Npr1 phosphorylation level (Figure 2A). A transient increase in the phosphorylation of Npr1, with a reduced mobility of the front line, was observed at time points 10 and 30 min, whereas a reduction in Npr1 phosphorylation was visible at 60 min. We estimated the impact of the phosphorylation level of Npr1 on its kinase activity by assessing the phosphorylation state of one of its targets, Amu1 (Figure 2B). Shifting cells to glucose-deprived medium resulted in the rapid dephosphorylation of Amu1 sustained even after 60 min, whereas shifting cells to fresh glucose-containing medium had no major impact on Amu1 phosphorylation state, suggesting that the kinase rapidly lost its activity upon glucose deprivation. Glucose re-supplementation after withdrawal induced a rapid phosphorylation of Amu1, indicating a fast recovery of Npr1 activity. Assuming that TORC1 is rapidly inactivated upon glucose withdrawal, these data suggest that the increased phosphorylation of Npr1 and its inactivation could occur independently of TORC1 activity. Some studies report that the Snf1 kinase mediates partial inhibition of TORC1 upon glucose withdrawal (Hughes Hallett et al., 2014, 2015). Npr1 appeared less abundant in Snf1-lacking cells grown in proline medium (Figure 2A). Moreover, we observed a clear impact of the absence of Snf1 on the Npr1 phosphorylation status. In Snf1-lacking cells, Npr1 phosphorylation upon glucose withdrawal lost its transient nature, increasing over time. No obvious dephosphorylation of Npr1 was observed after shifting *snf1Δ* cells to a fresh glucose-containing medium. These results suggest that Npr1 dephosphorylation could be impaired in the absence of Snf1.

In response to depriving an auxotrophic strain of the amino acid it is auxotrophic for, Gcn2 phosphorylates the Kog1 regulatory subunit of TORC1, leading to a downregulation of the TORC1 kinase activity (Yuan et al., 2017). We tested the potential involvement of Gcn2 in the regulation of Npr1 in response to the addition of preferred nitrogen sources, ammonium or glutamine, to cells growing with the non-preferred nitrogen source proline and in the absence of any auxotrophic stress. *GCN2* deletion did not prevent the apparent phosphorylation of Npr1 induced by ammonium and glutamine supplementation (Figure 2C).

These results indicate that glucose starvation and Snf1 control Npr1 phosphorylation level and activity.

### Npr1 Phosphorylation and Activity Are Controlled by Gtr1, Gtr2, and Pib2

In response to amino acid availability, TORC1 is regulated through the heterodimeric Gtr1 and Gtr2 GTPase complex, TORC1 being stimulated in the presence of GTP-bound Gtr1 and GDP-bound Gtr2 (Binda et al., 2009; Gong et al., 2011; Kira et al., 2014; Nicastro et al., 2017; Panchaud et al., 2013a). Interestingly, Npr1 phosphorylation and activity appear to be controlled by the Npr2 protein (Boeckstaens et al., 2014; Neklesa and Davis, 2009), a member of the SEACIT complex stimulating Gtr1 GTPase activity (Panchaud et al., 2013a, 2013b). To study the role of Gtr1 in the regulation of Npr1, we first followed the phosphorylation pattern of the kinase in response to glutamine and ammonium in *gtr1Δ* cells grown with proline (Figure 2D). As observed in the *snf1Δ* cells, Npr1 was sharply less abundant in the absence of Gtr1. By expressing *NPR1* under the control of the *MET25* promoter, we show that Npr1 is still less detected in the absence of Gtr1/2 or Snf1, indicating that the reduced quantity of Npr1 observed in the mutants is linked to a posttranscriptional effect (Figure S1). In response to ammonium or glutamine addition, the deletion of *GTR1* led to a delay in the appearance of Npr1 phosphorylation as well as to a smaller smear of phosphorylation (Figure 2D). Similar results were obtained in double *gtr1Δ gtr2Δ* cells, indicating that the induced Npr1 phosphorylation observed in the single *gtr1Δ* mutant is not linked to the activity of Gtr2 (Figure 2E). It was recently shown that the Gtr proteins control a pathway of endosome-to-plasma membrane protein recycling independently of TORC1 regulation (MacDonald and Piper, 2017). The absence of Gtr proteins might thereby impair the loading of the plasma membrane with transporters

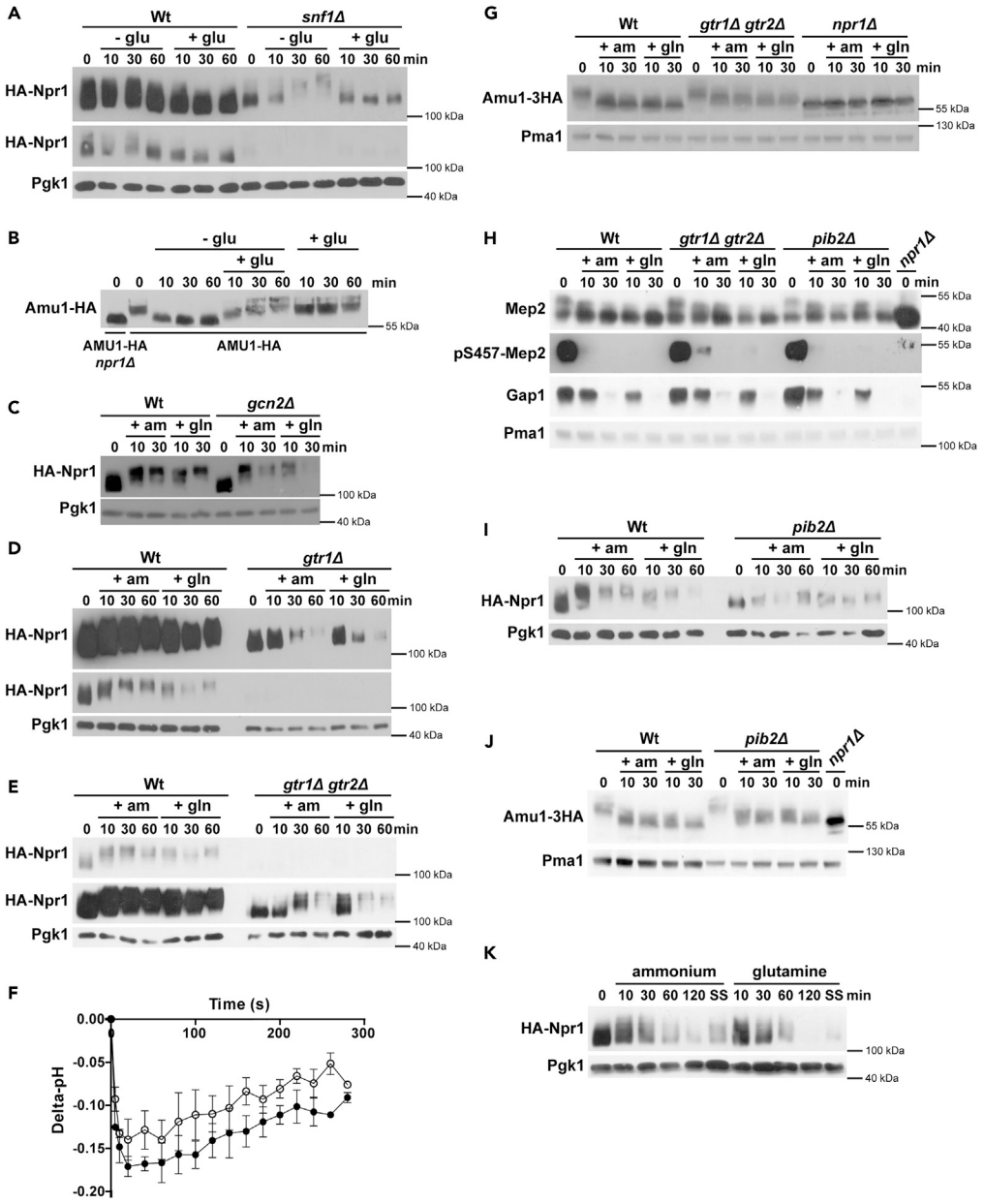


**Figure 2. Npr1 Phosphorylation and Activity Are Controlled by Snf1, Gtr1, Gtr2, and Pib2**

(A and B) (A) Immunodetection of HA-Npr1 from total extracts of proline-grown wild-type (23344c) and *snf1Δ* (PVV334) cells transformed with pAS103. At time 0, cells were shifted in a similar medium containing or not containing glucose 3%. Pgk1 was detected as a loading control. See also Figure S1. (B) Immunodetection of Amu1-HA from total extracts of proline-grown *AMU1-HA* (MB142) and *AMU1-HA npr1Δ* (36307b) cells transformed with pFL38. At time 0, cells were shifted in a similar medium containing or not containing glucose 3%. Glucose 3% was then added 60 min after glucose deprivation. (C–K) At time t = 0, glutamine 0.1% or ammonium 20 mM was added to the cell culture grown in the presence of proline as nitrogen source. Pgk1 or Pma1 was detected as loading controls in the immunodetection experiments.

(C) Immunodetection of HA-Npr1 from total extracts of wild-type (23344c) and *gcn2Δ* (MB383) cells transformed with pAS103.

(D) Immunodetection of HA-Npr1 from total extracts of wild-type (23344c) and *gtr1Δ* (PVV318) cells transformed with pAS103.

(E) Immunodetection of HA-Npr1 from total extracts of wild-type (23344c) and *gtr1Δ gtr2Δ* (MB386) cells transformed with pAS103. See also Figures S1 and S2A.

**Figure 2. *Continued***

(F) Evolution of $pH_c$ corrected for negative control variations (delta-pH) after addition of glutamine 0.1%. Data are represented as mean ± SEM (n = 2). Wild-type (23344c, ●) and *gtr1Δ gtr2Δ* (MB386, ○) cells were transformed with pYES-pHluorin and grown in the presence of proline as a nitrogen source.

(G) Immunodetection of Amu1-3HA from total extracts of wild-type (23344c), *npr1Δ* (30788a), and *gtr1Δ gtr2Δ* (MB386) cells transformed with YCpAmu1-3HA.

(H) Immunodetection of Mep2, pS457-Mep2, Gap1, and Pma1 from membrane-enriched extracts treated with N-glycosidase (F) Wild-type (23344c), *gtr1Δ gtr2Δ* (MB386), *pib2Δ* (PVV329), and *npr1Δ* (30788a) cells were transformed with pFL38.

(I) Immunodetection of HA-Npr1 from total extracts of wild-type (23344c) and *pib2Δ* (PVV329) cells transformed with pAS103. See also Figure S2.

(J) Immunodetection of Amu1-3HA from total extracts of wild-type (23344c), *npr1Δ* (30788a), and *pib2Δ* (PVV329) cells transformed with YCpAmu1-3HA.

(K) Immunodetection of HA-Npr1 from total extracts of *npr1Δ* (30788a) cells transformed with pAS103. These cells were also grown in the presence of ammonium 20 mM or glutamine 0.1% as nitrogen source (*SS*, steady-state culture).

and consequently the related nutrient uptake. To ensure that the delay in Npr1 phosphorylation was not due to a major delay in nitrogen entry in the *gtr1Δ gtr2Δ* strain, we compared the transient $pH_c$ drop accompanying glutamine addition in the presence and in the absence of Gtr1 and Gtr2. Glutamine-induced acidification was not significantly delayed in *gtr1Δ gtr2Δ* cells (Figure 2F), suggesting that glutamine is efficiently transported. We next determined whether the defect in Npr1 phosphorylation observed in cells lacking both Gtr proteins has an impact on the activity of the Npr1 kinase. Indeed, we previously showed that the link between the phosphorylated state of Npr1 and its activity is not straightforward (Boeckstaens et al., 2014). We therefore monitored the migration profile of three Npr1 targets, Amu1, Gap1, and Mep2 in *gtr1Δ gtr2Δ* cells (Figures 2G and 2H). Rapid Amu1 dephosphorylation occurred after ammonium or glutamine addition in wild-type and *gtr1Δ gtr2Δ* cells, consistent with a reduction of Npr1 activity in these conditions (Figure 2G). Nevertheless, the dephosphorylation appeared incomplete in the *gtr1Δ gtr2Δ* cells, the signal observed after ammonium or glutamine addition having a slower mobility compared with the signal observed in the absence of Npr1. Ammonium or glutamine supplementation triggered Gap1 degradation in both wild-type and *gtr1Δ gtr2Δ* cells, and dephosphorylation of the Mep2 serine 457 occurred in both strains even if it appeared slightly delayed in response to ammonium in the double mutant (Figure 2H). These results indicate that ammonium and glutamine supplementation leads to a large reduction of Npr1 activity in cells lacking Gtr1 and Gtr2 and that the latter proteins are not essential to transmit the inactivation signal to Npr1. It is noteworthy that, although Mep2 appears completely dephosphorylated and Gap1 degraded after glutamine supplementation to cells lacking the Gtr proteins, Amu1 remains partially phosphorylated. This suggests that Npr1 conserves a partial activity in these conditions and that this activity is target-specific.

We next considered the involvement of Pib2, another regulator of TORC1, in Npr1 control. It is still unclear whether Pib2 stimulates the activity of TORC1 in the same pathway or a pathway parallel to the one used by Gtr1 and Gtr2 GTPases (Kim and Cunningham, 2015; Michel et al., 2017; Tanigawa and Maeda, 2017; Ukai et al., 2018; Varlakhanova et al., 2017). Deletion of *PIB2* led to a net reduction of Npr1 phosphorylation induced by ammonium or glutamine addition, revealing a role of Pib2 in the regulation of Npr1 (Figure 2I). This Npr1 phosphorylation pattern was, however, different from the one observed in the absence of the Gtr proteins. Amu1 dephosphorylation still occurred in Pib2-lacking cells after ammonium or glutamine addition (Figure 2J). In the *pib2Δ* mutant, Amu1 dephosphorylation was, however, not complete. These data indicate that the activity of Npr1 is reduced in these conditions. *PIB2* deletion had no detectable effect on the Gap1 destabilization and the Mep2 S457 dephosphorylation observed upon glutamine or ammonium addition (Figure 2H). Our results indicate that cells deprived of Pib2 likely display a reduced activity of TORC1 upon preferred nitrogen source addition, leading to a weaker phosphorylation of Npr1. Nevertheless, the latter reduced Npr1 phosphorylation is sufficient to lead to a decrease of the kinase activity as deduced from the behavior of Npr1 targets.

Npr1 abundance is particularly reduced in Gtr-lacking cells, suggesting that the integrity of TORC1 might be required to regulate Npr1 stability (Figures 2E and S1). Of note, we observed that a longer-term incubation after supplementation of ammonium or glutamine resulted in a reduction of Npr1 abundance, suggesting a possible regulation of the Npr1 protein level (Figure 2K). Difference in steady-state levels of Npr1 further supports a varying abundance of Npr1 according to the quality of the nitrogen source. Furthermore, the glutamine-induced degradation of Npr1 seems to be reduced at 60 min specifically in the absence of Pib2 (Figures 2I and S2A). By monitoring the stability of Npr1 over a longer time, we show that the

degradation of Npr1 after glutamine addition is not prevented in the absence of Pib2 but is slightly delayed (Figures S2B and S2C).

Together, these results indicate that Pib2 and Gtr1/Gtr2 are involved in the TORC1-dependent regulation of Npr1 and that the presence of one of these two TORC1 regulators is sufficient to at least partially phosphorylate Npr1 and to reduce its activity upon glutamine or ammonium addition. It suggests that Pib2 and the Gtr proteins act in independent pathways to regulate TORC1 activity. Nevertheless, Gtr proteins and Pib2 differently regulate the phosphorylation state and the abundance of Npr1.

### Npr1 Inhibits TORC1 via Pib2

As Npr1 abundance appears to be controlled by the nitrogen source, we next addressed the impact of its expression level on growth efficiency. Npr1 is required for the activity of the three Mep ammonium transport proteins and to protect the general amino acid permease Gap1 from degradation, Gap1 notably ensuring citrulline transport (Boeckstaens et al., 2007, 2014, 2015; De Craene et al., 2001; Merhi and André, 2012). As expected, *npr1Δ* cells were unable to grow in the presence of citrulline or of low ammonium concentrations, as unique nitrogen sources (Figure 3A), as Gap1 and Mep proteins are not functional in the absence of the kinase (Boeckstaens et al., 2007; Dubois and Grenson, 1979; Grenson, 1983b). Expressing *NPR1* from the low-copy-number plasmid (YCpNpr1) restored the growth defect of *npr1Δ* cells on citrulline, whereas expression from the high-copy-number plasmid (YEpNpr1) appeared to slightly reduce this growth. Impairment of growth linked to *NPR1* overexpression was even more pronounced in the absence of Gtr1 and Gtr2, a condition reducing TORC1 activity. In the presence of the non-preferential nitrogen source citrulline, TORC1 is presumably poorly active. As observed in the presence of citrulline, growth on proline was also affected by *NPR1* overexpression, indicating that the Npr1-associated growth inhibition is not specific to citrulline (Table 1 and Figure 3A).

To test if *NPR1* overexpression could influence TORC1 activity, and thereby growth, we monitored the phosphorylation of the Rps6 TORC1 target in proline-grown cells upon glutamine addition. As expected, the glutamine-induced phosphorylation of Rps6 was reduced in the absence of the TORC1 activators, Pib2 or Gtr (Figures 3B and 3C). However, the Rps6 phosphorylation was not prevented in these mutants, indicating that Pib2 and Gtr act in independent pathways to regulate TORC1. Of note, high levels of *NPR1* expression did not significantly inhibit the Rps6 phosphorylation in the absence of Pib2, whereas expressing *NPR1* from a high-copy-number plasmid sharply reduced Rps6 phosphorylation in *npr1Δ gtr1Δ gtr2Δ* cells. These results suggest that Npr1 overproduction is able to impair TORC1 activation upon glutamine addition. Npr1 overproduction can reduce the TORC1 activation observable in the *npr1Δ gtr1Δ gtr2Δ* mutant but not the one detected in the *npr1Δ pib2Δ* cells. As the TORC1 activation observable in the cells deprived of Gtr1 and Gtr2 proceeds via Pib2 (Ukai et al., 2018), our results are consistent with TORC1 activity reduction upon Npr1 overproduction specifically relying on Pib2. Hence, our data suggest that, in conditions in which TORC1 is poorly active, overproduction of Npr1 is able to downregulate TORC1 via the Pib2 protein. Consistent with a role of Npr1 upstream of TORC1 and dependent on Pib2 and not on Gtr proteins, further deletion of *PIB2* did not affect the growth rate of *npr1Δ* cells in the presence of proline as nitrogen source contrary to the deletion of the *GTR* genes (Table 1).

Upstream activators of TORC1, such as components of the EGO complex, Gtr2 and Pib2, were notably discovered by screening the yeast gene knockout collection for mutants that exhibit a defect in recovery from rapamycin-induced inhibition of TORC1 (Dubouloz et al., 2005). Interestingly, *NPR1* deletion was described as suppressing the defect in exit from rapamycin-induced growth arrest of all three EGO mutants, as well as the one of the *gtr2Δ* cells. Our data indicate that deletion of *NPR1* suppressed the growth defect of the *gtr1Δ gtr2Δ* and *pib2Δ* cells during rapamycin recovery, suggesting that the kinase can act upstream of the TORC1 complex in this condition also independently of Pib2 (Figure 3D). Moreover, in agreement with a role of Npr1 in TORC1 inhibition, overproducing Npr1 reduced the growth recovery of cells after rapamycin treatment (Figure 3E).

Phosphoproteomic and large-scale interaction analyses report Pib2 as being differentially phosphorylated upon rapamycin treatment in Npr1-lacking cells compared with the wild-type strain and as physically interacting with the kinase (Fasolo et al., 2011; MacGurn et al., 2011). Accordingly, we observed a slightly faster mobility of the immunodetected GFP-Pib2 in the absence of Npr1, whereas the absence of Gtr1 and Gtr2 has no apparent effect on GFP-Pib2 mobility (Figures 4A and 4B). Moreover, alkaline phosphatase

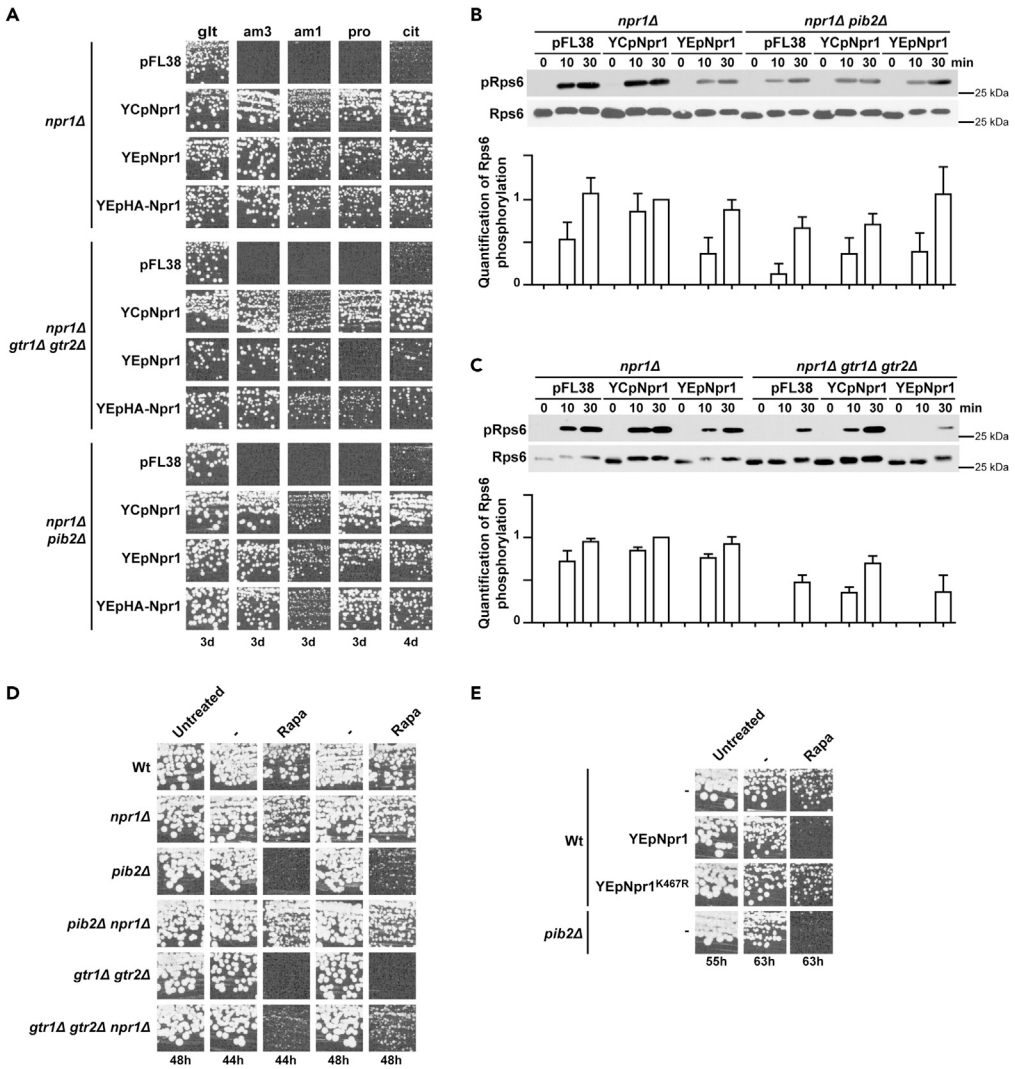


**Figure 3. Npr1 Inhibits TORC1 via Pib2**

(A–C) (A) Growth tests on minimal medium containing, as the sole nitrogen source, glutamate 0.1% (glt, positive growth control), proline 0.1% (pro), ammonium 1 (am1) or 3 (am3) mM, or citrulline 0.1% (cit). *npr1Δ* (PVV357), *pib2Δ npr1Δ* (PVV363), and *gtr1Δ gtr2Δ npr1Δ* (PVV366) cells were transformed with the empty vector pFL38, with the low-copy-number plasmid (YCpNpr1) or with the high-copy-number plasmids (YEpNpr1 and YEpHA-Npr1). The number of days of growth is indicated (*d*). (B and C) At time t = 0, glutamine 0.1% was added to the cell culture grown in the presence of proline as nitrogen source. Total Rps6 was detected as a loading control. Quantification of Rps6 phosphorylation was normalized using the corresponding total Rps6 signal. Data are represented as mean ± SEM (n = 3). (B) Immunodetection of pRps6 from total extracts of *npr1Δ* (PVV357) and *pib2Δ npr1Δ* (PVV363) cells transformed with pFL38, YCpNpr1, or YEpNpr1. (C) Immunodetection of pRps6 from total extracts of *npr1Δ* (PVV357) and *gtr1Δ gtr2Δ npr1Δ* (PVV366) cells transformed with pFL38, YCpNpr1, or YEpNpr1.

(D) Wild-type (23344c), *npr1Δ* (PVV357), *pib2Δ* (PVV329), *pib2Δ npr1Δ* (PVV363), *gtr1Δ gtr2Δ* (MB386), and *gtr1Δ gtr2Δ npr1Δ* (PVV366) cells were exposed to rapamycin (160 ng/mL) or to the rapamycin vehicle alone (-, ethanol/tween) for 3 h. Cells were then washed and plated on rich medium. Cells were imaged after 44 or 48 h of growth.

(E) *pib2Δ* (PVV329) cells transformed with the pFL38 empty plasmid (–), and wild-type (23344c) cells transformed with the pFL38 empty plasmid (–), YEpNpr1, or YEpNpr1$^{K467R}$ were exposed to rapamycin (160 ng/mL) or to the rapamycin vehicle alone (-, ethanol/tween) for 3 h. Cells were then washed and plated on minimal medium containing glutamine as nitrogen source. Cells were imaged after 55 or 63 h of growth.

treatment increased the mobility of Pib2 in wild-type cells (Figure 4B). These results indicate that Npr1 is required for Pib2 phosphorylation. We next studied the influence of the nitrogen source quality on Pib2 mobility. Glutamine was added to proline-grown cells for 1 h, and cells were then transferred to a proline

| Plasmids | Wild-type (23344c) | *npr1Δ* (PVV357) | *pib2Δ npr1Δ* (PVV363) | *gtr1Δ gtr2Δ npr1Δ* (PVV366) |
|---|---|---|---|---|
| pFL38 | 3h04 | 6h35 | 6h12 | 7h24 |
| YCpNpr1 | ND | 3h07 | 3h08 | 3h22 |
| YEpNpr1 | ND | 3h48 | 4h20 | 7h46 |
| YEpHA-Npr1 | ND | 3h46 | 4h19 | 5h41 |

**Table 1. Generation Doubling Time of Different Strains Growing in Liquid Minimal Medium Containing Proline as Nitrogen Source**
ND, not determined.

medium. Glutamine supplementation slightly increased the mobility of Pib2, whereas transferring the cells to proline reduced the mobility of the protein (Figure 4C). These differences in Pib2 mobility were not observed in Npr1-lacking cells, suggesting that the kinase controls Pib2 phosphorylation according to the quality of the nitrogen supply.

GFP-Pib2 was shown as localized at the vacuolar and endosomal membranes and also as vacuole-associated puncta under nitrogen starvation (Hatakeyama et al., 2019; Ukai et al., 2018). We observed that, in the presence of proline, a poor nitrogen supply, the proportion of cells containing GFP-Pib2 puncta is slightly increased in the absence of the Npr1 kinase (*npr1Δ*: 81% versus Wt: 71%, $p < 0.02$) (Figure 4D). Remarkably, we observed a strong vacuolar fragmentation in the absence of the Npr1 kinase in proline-grown cells expressing GFP-Pib2 (*npr1Δ*: 37% of cells containing fragmented vacuole versus Wt: 7%, $p < 10^{-3}$). Addition of glutamine (1 h) to proline-grown *npr1Δ* cells sharply reduced the proportion of cells containing fragmented vacuoles (*npr1Δ* glutamine: 13% versus *npr1Δ* proline: 37%, $p < 10^{-3}$).

Overall, our data indicate that TORC1 inhibition by Npr1 is dependent on Pib2 and that the kinase influences the phosphorylation state of Pib2 and has a minor impact on its localization as puncta at the vacuolar membrane.

## The N-Terminal Regulatory and the C-Terminal Catalytic Domains of the Bipartite Npr1 Kinase Are Involved in Distinct Functions

Npr1 is composed of two domains: an N-terminal S-rich domain, the target of extensive phosphorylation, and a C-terminal catalytic domain (Gander et al., 2008; Vandenbol et al., 1990). To determine if the N-terminal domain is required for Npr1 function and/or for its regulation, we constructed two versions of GFP-tagged protein with the N-terminal domain removed. A first construction (414-Start) corresponds to the deletion of the 413 N-terminal Npr1 amino acids as defined by Gander and collaborators (Gander et al., 2008). In the second truncated Npr1, the first 437 amino acids (438-Start) are deleted, being limited to the catalytic kinase domain as defined by Prosite (https://prosite.expasy.org/). The Npr1 variants are detected at the expected molecular weight but the 438-Start variant of Npr1 appears slightly less stable than the native and the 414-Start versions (Figures 5A and S3). Although GFP-Npr1 was efficiently phosphorylated in response to glutamine addition, no apparent modification of the N-truncated Npr1 was observed, showing that the N-terminal part of the protein is a major target of glutamine-induced phosphorylation in agreement with a previous study (Gander et al., 2008) (Figure 5A). As shown in Figure 5B, both N-truncated Npr1 variants were able to restore growth of *npr1Δ* cells on low ammonium concentrations and at least partially on citrulline, revealing that N-truncated Npr1 is able to restore the activity of Gap1 and at least of one of the Mep proteins. Western blot experiments show that deletion of the N-terminal extremity of Npr1 led to a partial degradation of Gap1 and to an absence of phosphorylation of Mep2 on S457 (Figure 5C). As the truncated Npr1 variants are able to ensure growth on ammonium, the latter observation is consistent with these Npr1 variants restoring Mep1 and Mep3 activity by inhibiting Amu1 while being unable to restore Mep2 activity. Accordingly, N-truncated Npr1 variants are able to at least partially ensure Amu1 phosphorylation (Figure 5D).

Surprisingly, we observed that, in proline medium, *gtr1Δ gtr2Δ npr1Δ* cells overproducing HA-Npr1 grew better than cells overproducing native Npr1 (Figure 3A and Table 1). HA-tagging of Npr1 at its N-terminus has an inhibitory effect on Npr1 function, especially in the absence of Gtr (Table 1). Accordingly, in the

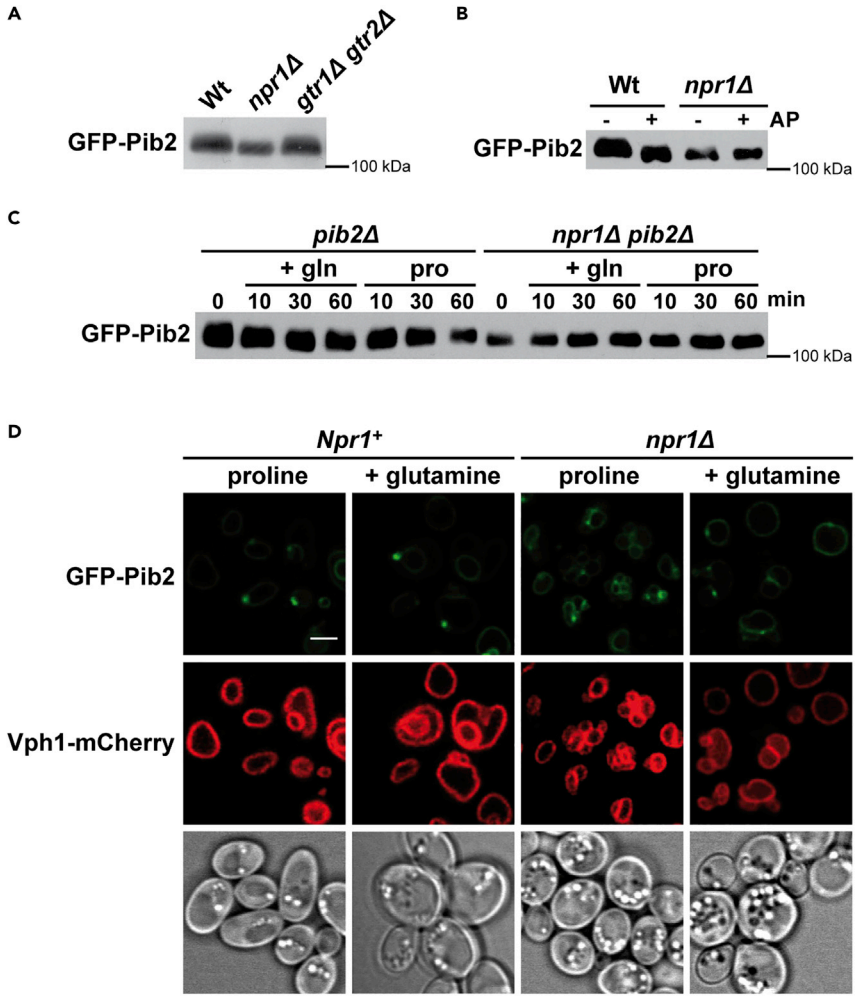


**Figure 4. Npr1 Controls Pib2 Phosphorylation**

(A) Immunodetection of GFP-Pib2 from total extracts of proline-grown wild-type (23344c), *npr1Δ* (30788a), and *gtr1Δ gtr2Δ* (MB386) cells transformed with the plasmid YCpGFP-Pib2.

(B) Immunodetection of GFP-Pib2 from total extracts treated (+) or not treated (−) with alkaline phosphatase. Proline-grown wild-type (23344c) and *npr1Δ* (30788a) cells were transformed with the plasmid YCpGFP-Pib2.

(C) Immunodetection of GFP-Pib2 from total extracts of wild-type (23344c) and *npr1Δ* (30788a) cells transformed with the plasmid YCpGFP-Pib2. At time 0, glutamine (0.1%) was added to the cell culture grown in the presence of proline as nitrogen source. One hour after glutamine addition, cells were transferred in a minimal medium containing proline as nitrogen source.

(D) Vph1-mCherry (MB393) and Vph1-mCherry *npr1Δ* (PVV353) cells transformed with the plasmid YCpGFP-Pib2 were visualized by fluorescence microscopy. Cells were grown in the presence of proline, and then glutamine 0.1% was added during 1 h. Scale bar, 2 μm.

*gtr1Δ gtr2Δ* mutant, N-terminal HA-tagging of Npr1 at least partially masked the negative impact of the kinase overproduction on Rps6 phosphorylation, suggesting that HA-tagging could reduce the TORC1-inhibiting function of Npr1 in these conditions (Figure 5E). HA-tagged Npr1 thus appears less efficient than native Npr1 in TORC1 inhibition. The HA tag might for instance perturb the integrity of the N-terminal part of Npr1 and thereby alter the Pib2-dependent inhibition of TORC1. To test if the C-terminal catalytic activity of the Npr1 kinase is involved in the inhibition of TORC1, we constructed a version of Npr1 mutated in the catalytic domain (K467R) (Crespo et al., 2004; Gander et al., 2008). As GFP-Npr1, the kinase-dead K467R version was efficiently phosphorylated in response to glutamine addition, indicating that the observed phosphorylation is not linked to auto-phosphorylation (Figure 5A). This mutated form of Npr1, however, appears less abundant than the native form (Figures 5A and S3). Npr1$^{K467R}$ is unable to ensure Mep2 phosphorylation and to prevent Gap1 degradation, confirming that the kinase lost the catalytic

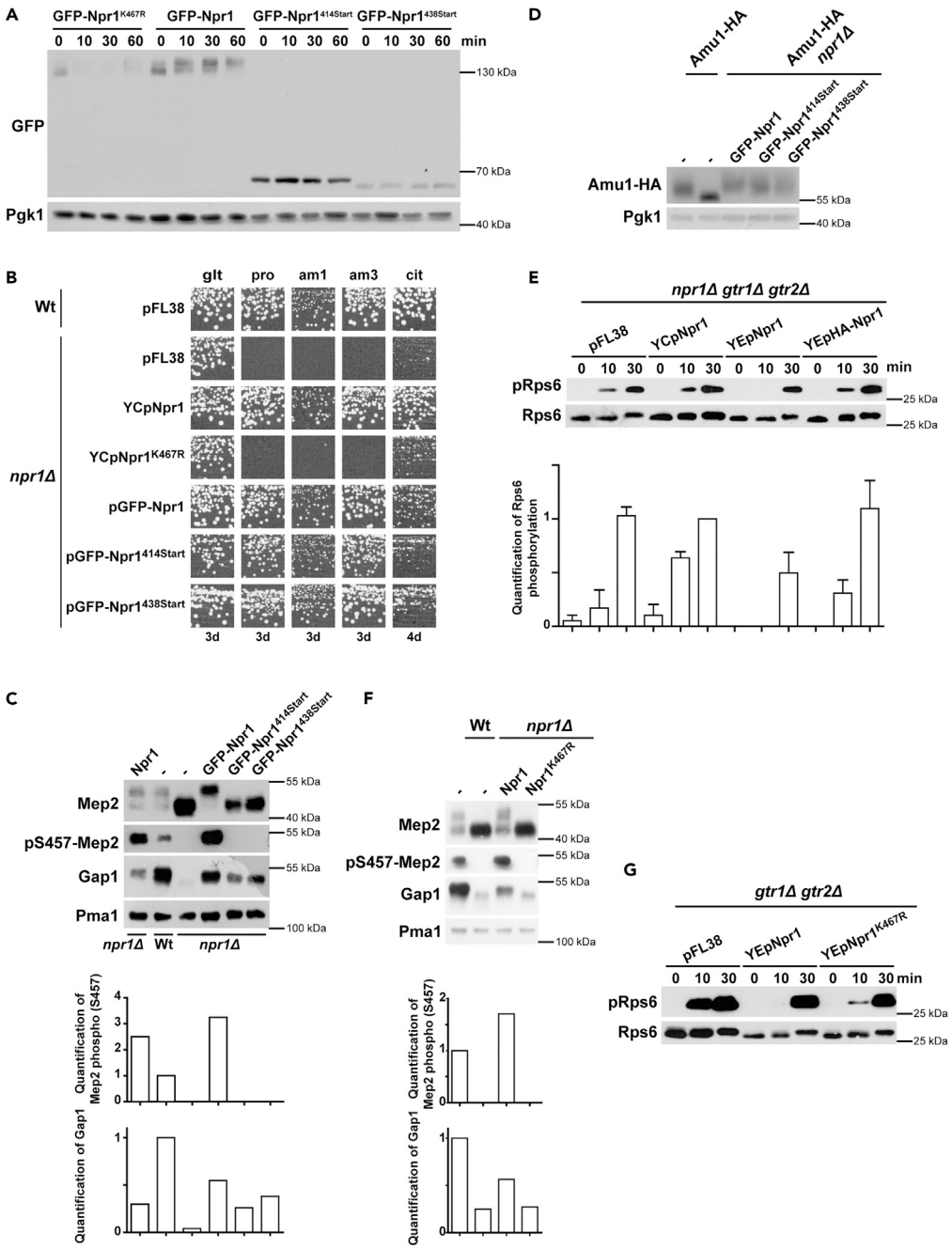


**Figure 5. The N-terminal Regulatory and the C-terminal Catalytic Domains of Npr1 Are Involved in Distinct Functions**

(A) Immunodetection of GFP-Npr1, GFP-Npr1$^{414Start}$, GFP-Npr1$^{438Start}$, and GFP-Npr1$^{K467R}$ from total cellular extracts. Proline-grown *npr1Δ* (PVV357) cells were transformed with the plasmids YCpGFP-Npr1, YCpGFP-Npr1$^{414Start}$, YCpGFP-Npr1$^{438Start}$, or YCpGFP-Npr1$^{K467R}$. See also Figure S3.

(B) Growth tests on minimal medium containing, as the sole nitrogen source, proline 0.1% (pro), ammonium 1 (am1) or 3 (am3) mM, citrulline 0.1% (cit), or glutamate 0.1% (glt, positive growth control). Wild-type (23344c) cells were transformed with the empty vector pFL38 and, *npr1Δ* (PVV357) cells with the empty vector pFL38, or with YCpNpr1, YCpNpr1$^{K467R}$, YCpGFP-Npr1, YCpGFP-Npr1$^{414Start}$, or YCpGFP-Npr1$^{438Start}$. The number of days of growth is indicated (*d*).

(C) Immunodetection of Mep2, pS457-Mep2 and Gap1 from membrane-enriched extracts treated with N-glycosidase F Pma1 was detected as a loading control. Wild-type (23344c) cells transformed with the empty vector pFL38 and, *npr1Δ* (PVV357) cells transformed with the empty vector pFL38, or with YCpNpr1, YCpGFP-Npr1, YCpGFP-Npr1$^{414Start}$, or

**Figure 5. *Continued***

YCpGFP-Npr1$^{438Start}$ were grown in the presence of proline as nitrogen source. Quantifications of Mep2 phosphorylation and of Gap1 abundance were normalized using the loading control Pma1 signal.

(D) Immunodetection of Amu1-HA from total extracts of *AMU1-HA* (MB142) and *AMU1-HA npr1Δ* (36307b) cells transformed with the empty vector pFL38, or with YCpGFP-Npr1, YCpGFP-Npr1$^{414Start}$, or YCpGFP-Npr1$^{438Start}$. Cells were grown in the presence of proline as nitrogen source. Pgk1 was detected as loading control.

(E) Immunodetection of pRps6 from total extracts of *gtr1Δ gtr2Δ npr1Δ* (PVV366) cells transformed with the empty vector pFL38, with the low-copy-number plasmid (YCpNpr1) or with the high-copy-number plasmids (YEpNpr1 and YEpHA-Npr1). Total Rps6 was detected as a loading control. At time 0, glutamine (0.1%) was added to the cell culture grown in the presence of proline as nitrogen source. Quantification of Rps6 phosphorylation was normalized using the corresponding total Rps6 signal. Data are represented as mean ± SEM (n = 3).

(F) Immunodetection of Mep2, pS457-Mep2, and Gap1 from membrane-enriched extracts treated with N-glycosidase F Pma1 was detected as a loading control. Wild-type (23344c) cells transformed with the empty vector pFL38 and, *npr1Δ* (PVV357) cells transformed with the empty vector pFL38, or with YCpNpr1, or YCpNpr1$^{K467R}$ were grown in the presence of proline as nitrogen source. Quantifications of Mep2 phosphorylation and of Gap1 abundance were normalized using the loading control Pma1 signal.

(G) Immunodetection of pRps6 from total extracts of *gtr1Δ gtr2Δ* (MB386) cells transformed with the empty vector pFL38, or with the high-copy-number plasmids (YEpNpr1 and YEpNpr1$^{K467R}$). Total Rps6 was detected as a loading control. At time 0, glutamine (0.1%) was added to the cell culture grown in the presence of proline as nitrogen source.

function (Figure 5F). Accordingly, cell growth ensured by Npr1$^{K467R}$ is sharply reduced compared with the growth ensured by native Npr1 in the presence of a low ammonium concentration or of citrulline as nitrogen sources (Figure 5B). Expressing *NPR1$^{K467R}$* from a high-copy-number plasmid reduced Rps6 phosphorylation in *gtr1Δ gtr2Δ* cells but slightly less efficiently than expressing native *NPR1* (Figure 5G). In the same way, expressing *NPR1$^{K467R}$* from a high-copy-number plasmid sharply reduced growth in the presence of proline of the *gtr1Δ gtr2Δ* cells, even if the growth impairment was not as strong as by expressing native *NPR1* (*gtr1Δ gtr2Δ* + pFL38: 3h27; *gtr1Δ gtr2Δ* + YEpNpr1: 7h15; *gtr1Δ gtr2Δ* + YEpNpr1$^{K467R}$: 5h25). The slighter effects of the K467R variant could be attributable to a reduction of the stability of the protein. These data reveal that TORC1 inhibition mediated by Npr1 is largely independent of the kinase catalytic function and suggest a role of the N-terminal extremity of Npr1 in this function.

We previously observed that overproducing Npr1 inhibits the recovery of cells after rapamycin treatment, suggesting a role of the kinase upstream of TORC1 (Figure 3E). The inhibitory effect of *NPR1* overexpression is alleviated by the presence of the catalytic mutation (K467R), revealing that the catalytic function of Npr1 is required to inhibit TORC1 in this particular context.

Overall, our data indicate that the N-terminal non-catalytic domain of the bipartite Npr1 kinase plays a key role in the control of specific targets and is required for TORC1 inhibition in particular contexts.

## DISCUSSION

The TORC1 signaling network is a major regulator of cell growth in all eukaryotes. This network is activated by various signals, such as amino acids, glucose, and also growth factors in mammalian cells (De Virgilio and Loewith, 2006; Eltschinger and Loewith, 2016; González and Hall, 2017; Howell et al., 2013; Loewith and Hall, 2011; Shimobayashi and Hall, 2014; Wullschleger et al., 2006). In this study, we first evaluated the role of pH as a general signal regulating TORC1. A genome-wide analysis revealed that $pH_c$ controls cell growth (Orij et al., 2012). Of note, the V-ATPase is proposed to behave as a pH sensor regulating not only TORC1 but also Ras/PKA, likely by interacting with Gtr1 and Arf1, two GTPases, respectively, required for the activation of these pathways (Dechant et al., 2014). In mammalian cells, the V-ATPase appears to also modulate the activity of mTORC1 in response to leucine (Zoncu et al., 2011). In a former work, we similarly proposed that the fungal Mep2 ammonium transport protein, which is also qualified as a sensor but in the context of pseudohyphal growth induction, could allow filamentation via a specific transport mechanism leading to an intracellular pH modification in turn impacting signaling pathways (Boeckstaens et al., 2008). These considerations prompted us to evaluate a role of pH as a signal controlling TORC1 in response to $H^+$-coupled transport of nitrogen sources. Nitrogen addition triggers a transient rapid drop in $pH_c$ with an extent that does not reflect the quality of the nitrogen source. There is no correlation between the pH variation, the added nitrogen source expected to lead to a modification of the growth rate, and the apparent extent of the associated Npr1 phosphorylation. Furthermore, cytosolic acidification, by shifting cells at pH 2.3 or by adding acetic acid, does not efficiently activate TORC1. In line with these results, cytosolic acidification accompanying glucose

withdrawal or supplementation of the CCCP protonophore inhibits TORC1 (Kawai et al., 2011; Orij et al., 2012; Prouteau et al., 2017). In addition, TORC1 activation can occur upon ammonium supplementation to triple-*mepΔ* cells despite associated cytosolic basification. Even if the transient $pH_c$ decrease associated with amino acid or ammonium transport could transiently activate TORC1, whatever the quality of the nitrogen supply, our results show that cytosolic acidification is not a prerequisite for TORC1 activation. Of note, in mammalian cells, mTORC1 activity is inhibited by acidification (Balgi et al., 2011; Fonseca et al., 2012). Furthermore, $pH_c$ decrease is correlated to yeast growth impairment (Orij et al., 2012).

We further highlighted that glucose withdrawal, known to be accompanied by cytosolic acidification, results in at least a transitory Npr1 phosphorylation and inactivation. If TORC1 is inactivated in this condition (Prouteau et al., 2017), it suggests that Npr1 could be regulated by another kinase according to glucose availability. Alternatively, or in addition, the phosphatase responsible for Npr1 dephosphorylation could be inactivated. Our data support a role of the Snf1 kinase in the control of Npr1 phosphorylation and activity, in response to glucose availability. We observed that the Npr1 phosphorylation, induced by glucose deprivation, loses its transient nature in Snf1-lacking cells, suggesting a role of Snf1 in the control of the phosphorylation level of Npr1. Contradictory hypotheses are reported in the literature concerning the role of Snf1, a homologue of mammalian AMP-activated protein kinase (AMPK), in contributing to TORC1 inhibition upon glucose withdrawal (Hughes Hallett et al., 2014, 2015; Prouteau et al., 2017).

Several proteins, including the Gtr1 and Gtr2 GTPases, Pib2, and the Gcn2 kinase, have been proposed to mediate the nitrogen and/or amino acid signal to TORC1, whereas their exact contribution and operating conditions remain unclear (Dubouloz et al., 2005; Kim and Cunningham, 2015; Michel et al., 2017; Tanigawa and Maeda, 2017; Varlakhanova et al., 2017). These regulators could differently control TORC1 leading to various outcomes on the targets of the complex. Gcn2 was recently proposed to phosphorylate the Kog1 regulatory subunit of TORC1, resulting in downregulation of TORC1 kinase activity in response to amino acid starvation, namely, upon leucine or histidine starvation in a *leu2 his3* auxotrophic strain (Yuan et al., 2017). The Gcn2 kinase does not seem to intervene in response to the starvation of the major nitrogen source, suggesting that the kinase could regulate TORC1 in particular conditions of amino acid deficiency specific to auxotrophic strains. Accordingly, we found no apparent influence of Gcn2 on the phosphorylation status of the TORC1 effector Npr1 in the ammonium or amino acid supplementation experiments performed in prototrophic conditions. On the other hand, although a recent work proposes that the presence of both Pib2 and Gtr GTPases is strictly required for glutamine-dependent TORC1 activation, other studies conclude that these proteins act through independent pathways to activate TORC1 (Kim and Cunningham, 2015; Michel et al., 2017; Ukai et al., 2018; Varlakhanova et al., 2017). Our data, obtained using the Σ1278b background in prototrophic conditions, support the latter view indicating that Pib2 and the Gtr complex both participate in the activation of TORC1 in response to amino acid and ammonium addition to proline-grown cells (Figure 6). The discrepancies with the work of Varlakhanova and collaborators might result from the experimental conditions, as auxotrophic strains were used in the absence of the complementing amino acids, a specific condition in which the Gcn2 kinase is able to inactivate TORC1 (Varlakhanova et al., 2017). In this condition of Gcn2-mediated inhibition, both Gtr and Pib2 might be simultaneously required to ensure TORC1 activation. In agreement with the model of two independent pathways, synthetic lethality is observed when *GTR1* and *PIB2* genes are simultaneously deleted (Kim and Cunningham, 2015). Although both are required for TORC1 activation, we found that Gtr proteins and Pib2 regulate the phosphorylation state and the abundance of Npr1 in different ways. Importantly, unlike Pib2, Gtr proteins are involved in the control of Npr1 abundance. We also observed that ammonium- or glutamine-induced phosphorylation of Npr1 is largely reduced in *pib2Δ* cells, whereas it is delayed and reduced in *gtr1Δ gtr2Δ* cells. This delay in Npr1 phosphorylation does not appear to be attributable to an ineffective entry of the nitrogen source in the absence of Gtr1 and Gtr2. The correlation between hyperphosphorylation of Npr1 and inactivation of the kinase activity is not so straightforward. Despite its hyperphosphorylated state in the absence of the Sit4 phosphatase, Npr1 is still able to mediate Mep2 phosphorylation (Boeckstaens et al., 2014). We therefore used three independent readouts to test Npr1 kinase activity. Ammonium and glutamine supplementation to cells lacking either Pib2 or Gtr1 and Gtr2 still leads to a large reduction of Npr1 activity, even if the kinase appears only partially phosphorylated in these conditions. Either pathway is thus sufficient to transmit the inactivation signal to Npr1. Distinct phosphorylation sites controlled by either Pib2 or Gtr could exist in Npr1. Although the Npr1 kinase appears inactivated after glutamine supplementation in the absence of the Gtr or Pib2 proteins considering the Mep2 and Gap1 targets, a basal Amu1 phosphorylation is still observed. This suggests that the partial activity of Npr1 in these conditions is target specific. Both

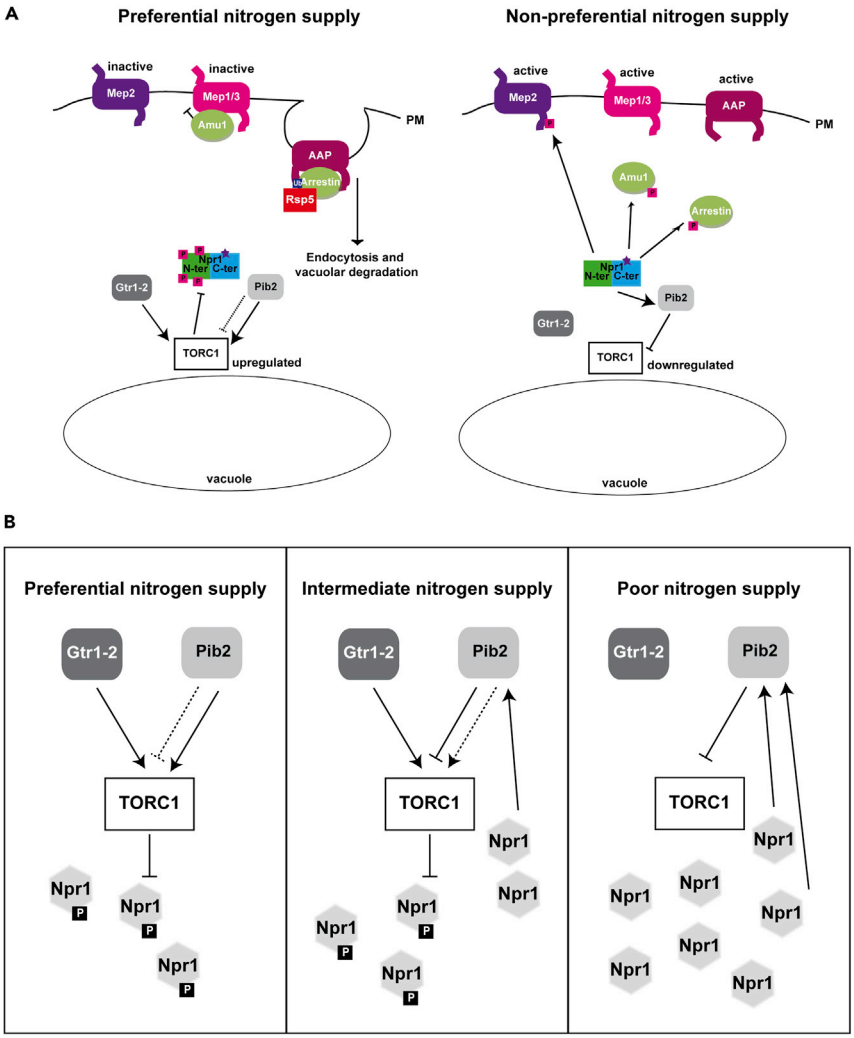


**Figure 6. Model of the Feedback Control of TORC1 by Its Npr1 Effector**

(A) Upon preferred nitrogen supplementation, Pib2 and the Gtr proteins activate TORC1, and Npr1 is hyperphosphorylated and inhibited. Under these conditions, Amu1 is dephosphorylated and accumulates at the cell surface and mediates inhibition of ammonium transport through Mep1 and Mep3. The non-phosphorylated autoinhibitory domain of Mep2 prevents the enhancer domain to activate the transport protein. Dephosphorylated arrestin-like adaptors recruit the Rsp5 ubiquitin-ligase to their permease targets, which are ubiquitylated, endocytosed, and degraded in the vacuole. Upon non-preferred nitrogen supply, TORC1 is poorly active and Npr1 is hypophosphorylated and active. Npr1 is able to efficiently reduce the slight activity of TORC1 and mediate the phosphorylation of its different targets. Npr1 mediates the phosphorylation of Amu1, which remains cytosolic, whereas Mep1 and Mep3 are kept active. Npr1 enables C-terminal phosphorylation of the Mep2 ammonium transport protein, thereby silencing an autoinhibitory domain and allowing Mep2 activity. Npr1 mediates phosphorylation of arrestin-like adaptors thereby protecting their permease targets from endocytosis and vacuolar degradation. The catalytic function of Npr1 is represented by a star.

(B) Upon preferred nitrogen supplementation, TORC1 is rapidly activated and induces the phosphorylation and the inactivation of Npr1. In case of strong nitrogen signal in terms of quality and quantity, Npr1 is largely inactivated and would be unable to inhibit TORC1. If the signal is moderate, Npr1 could conserve an intermediate activity and would thereby downregulate TORC1 via Pib2, reducing the activity of the TORC1 network and in turn regulating its own activity. In condition of poor nitrogen supply, TORC1 is poorly active and Npr1 is active and able to efficiently reduce the slight activity of TORC1. This feedback loop would lead to a more efficient downregulation of TORC1 and to a faster re-activation of TORC1 in response to a novel signal.

non-preferential and preferential nitrogen sources were shown to induce a rapid and transient Gtr-dependent peak of TORC1-Sch9 activity, whereas only the preferential nitrogen sources provoke a second sustained, likely Gtr-independent, peak (Stracka et al., 2014). The delay we observed in Npr1 phosphorylation in Gtr-lacking cells could correspond to the absence of the first TORC1 activation peak. Alternatively, it could simply illustrate that the transmission of the signal is reduced and delayed.

Our results also indicate a regulation of Npr1 stability according to the quality of the nitrogen supply as the kinase abundance decreases in the presence of ammonium or glutamine. However, in these conditions, Npr1 is still active as cells lacking the kinase show a detectable delay of growth on ammonium 20 mM, for instance, and a basal kinase activity is retained (Boeckstaens et al., 2007; Gander et al., 2008). Npr1 is structured into an N-terminal serine-rich domain predicted to contain PEST sequences and a C-terminal catalytic kinase region (Vandenbol et al., 1990). Phosphorylation of PEST regions is reported to constitute a signal for protein degradation (Rechsteiner and Rogers, 1996). Interestingly, Npr1 abundance appears sharply reduced in the absence of Gtr or Snf1 specifically but remains normal in the absence of Pib2. This difference in Npr1 abundance is linked to a posttranscriptional effect suggesting that Gtr and Snf1 can control the protein stability. In the absence of Ptc1, an effector phosphatase and a potential regulator of TORC1, Npr1 appears hyperphosphorylated and also less abundant than in wild-type cells (González et al., 2009). The presence of specific proteins in complex with Npr1 might be required to protect it from degradation according to the nitrogen quality signal. Moreover, we observed that the C-terminal catalytic domain of Npr1 is sufficient to ensure Gap1 stability and Mep1-Mep3 activities, whereas the N-terminal PEST domain is sensitive to regulation by glutamine and is required for Mep2 phosphorylation and activity (Figure 6A).

Our data suggest an inhibitory role of Npr1 upstream of TORC1. Npr1 overproduction has a negative impact on yeast growth and on the TORC1 activation, as revealed by the reduction of Rps6 phosphorylation after glutamine addition and by the defect of cell recovery after rapamycin treatment. After glutamine supplementation to proline-grown cells, the negative effect of Npr1 overproduction is highlighted in conditions of low TORC1 activity and predominantly in Gtr-lacking cells but is lost in the absence of Pib2. This suggests that Pib2 is required for Npr1-dependent downregulation of TORC1 in this condition. Nevertheless, our data support previous studies showing that *NPR1* deletion suppresses the defect of *gtrΔ* and *pib2Δ* cells to recover after rapamycin treatment, suggesting a role of Npr1 upstream of TORC1 also independently of Pib2 (Dubouloz et al., 2005; Varlakhanova et al., 2017). The catalytic function of Npr1 is not strictly required for the inhibition of glutamine-dependent Rps6 phosphorylation linked to Npr1 overproduction, whereas this function is necessary to inhibit the defect of growth recovery after rapamycin treatment. This suggests that Npr1 could differently inhibit distinct functions of TORC1 according to the stimulus and at least one of these requires the presence of Pib2. Npr1 might impact on TORC1 activity via other effectors in the condition of rapamycin recovery. Of note, the chromosomal locus of Amu1/Par32 was identified as being required for rapamycin recovery by Dubouloz and collaborators, an observation later confirmed by Varlakhanova and co-workers, thus placing Amu1/Par32 upstream of TORC1 (Dubouloz et al., 2005; Varlakhanova et al., 2018). Hence, as inhibitory phosphorylation of Amu1 is controlled by Npr1 (Boeckstaens et al., 2015), the kinase could also act upstream of TORC1 via Amu1. Consistent with a different TORC1 activation in function of the stimulus, Pib2 and Gtr proteins are both independently required for cell recovery after rapamycin treatment but the presence of only one is sufficient to induce the phosphorylation of Npr1 or Rps6 upon glutamine or ammonium addition.

Physical interactions are reported for Npr1 with all the TORC1 subunits, as well as with TORC1 regulators, notably including Pib2 but also the negative regulators Gcn2 and Snf1 (Breitkreutz et al., 2010; Fasolo et al., 2011). Npr1 could downregulate TORC1 by sequestering Pib2 and by preventing Pib2 to activate TORC1. Pib2 is differentially phosphorylated upon rapamycin treatment in Npr1-lacking cells (MacGurn et al., 2011). We show here that the phosphorylation status of Pib2 varies according to the quality of the nitrogen supply in a Npr1-dependent manner. Almost all reported phosphorylated sites in Pib2 are located in the N-terminal part associated with the negative TORC1 regulation (Albuquerque et al., 2008; Gnad et al., 2009; Holt et al., 2009; Huber et al., 2009). Moreover, Npr1 does not seem to majorly influence the localization of GFP-Pib2 at the vacuolar membrane and as puncta associated with this membrane. The enhanced localization of Pib2 as puncta in the absence of the kinase could be linked to a more starved state of the *npr1Δ* cells. Unexpectedly, we observed an impressive proportion of cells displaying fragmented vacuoles specifically in *npr1Δ* cells overproducing GFP-Pib2, still suggesting a tangle between the functions of Npr1 and Pib2. It has been proposed that TORC1 stimulates vacuole fragmentation in a Sit4-dependent way

(Michaillat et al., 2012). Pib2 and Npr1, a known target of Sit4 (Boeckstaens et al., 2014; Di Como and Arndt, 1996; Jacinto et al., 2001), could be involved in the TORC1-controlled process of vacuole fragmentation.

It is tempting to propose that Npr1 is part of a large multiprotein complex, including TORC1 and its regulators, in which Npr1 activity would be tuned by TORC1-dependent phosphorylation. Npr1 would in turn exert a feedback control on TORC1. This feedback control would balance TORC1 activity and involve the N-terminal extremity of Pib2. The regulation of TORC1 by its Npr1 effector could constitute a feedback loop (Figure 6B). In conditions of preferred and abundant nitrogen supplementation, TORC1 is rapidly activated and induces the phosphorylation and the inactivation of Npr1. In case of strong nitrogen signal in terms of quality and quantity, Npr1 will be largely inactivated and turned unable to inhibit TORC1. If the signal is moderate, Npr1 could conserve an intermediate activity and thereby downregulate TORC1 via Pib2, reducing the activity of the TORC1 network and in turn regulating its own activity. This feedback loop could lead, in the case of a moderate signal, to a more efficient downregulation of TORC1 and a faster re-activation of TORC1 in response to a novel signal.

### Limitations of the Study

In this study, we used artificial conditions by overexpressing the *NPR1* gene to study the effect of Npr1 abundance on TORC1 activity. This overexpression allowed us to highlight a negative regulation of TORC1 by Npr1, but we must bear in mind that the artificial overexpression of proteins could drive effects not observed in natural conditions.

## METHODS

All methods can be found in the accompanying Transparent Methods supplemental file.

## SUPPLEMENTAL INFORMATION

Supplemental Information can be found online at https://doi.org/10.1016/j.isci.2019.09.025.

## ACKNOWLEDGMENTS

We thank Jérôme Savocco and Gordon Williamson for critical reading of the manuscript. We thank Johannes Hegemann for sharing materials (pUG36). A.S.B. is a research fellow of the F.R.S.-FNRS, S.S.D. is recipient of an FRIA fellowship of the F.R.S.-FNRS, M.B. is a scientific research worker supported by ARC and WELBIO, and A.M.M. is a senior research associate of the F.R.S.-FNRS and a WELBIO investigator. This work was supported by F.R.S.-FNRS (CDR J017617F, PDR T011515F, PDR T.0160.19), ARC, WELBIO, the Brachet Funds, and the "Alice et David Van Buuren" foundation.

## AUTHOR CONTRIBUTIONS

M.B. and A.M.M. conceived and designed the experiments. M.B., A.S.B., S.S.D., and P.V.V. performed the experiments. P.G., M.B., and A.M.M. analyzed the data. M.B. and A.M.M. wrote the paper.

## DECLARATION OF INTERESTS

The authors declare no competing interests.

Received: August 15, 2018
Revised: May 10, 2019
Accepted: September 13, 2019
Published: October 25, 2019

## REFERENCES

Albuquerque, C.P., Smolka, M.B., Payne, S.H., Bafna, V., Eng, J., and Zhou, H. (2008). A multidimensional chromatography technology for in-depth phosphoproteome analysis. Mol. Cell. Proteomics *7*, 1389–1396.

Balgi, A.D., Diering, G.H., Donohue, E., Lam, K.K.Y., Fonseca, B.D., Zimmerman, C., Numata, M., and Roberge, M. (2011). Regulation of mTORC1 signaling by pH. PLoS One *6*, e21549.

Beck, T., and Hall, M.N. (1999). The TOR signalling pathway controls nuclear localization of nutrient-regulated transcription factors. Nature *402*, 689–692.

Binda, M., Péli-Gulli, M.-P., Bonfils, G., Panchaud, N., Urban, J., Sturgill, T.W., Loewith, R., and De Virgilio, C. (2009). The Vam6 GEF controls TORC1 by activating the EGO complex. Mol. Cell *35*, 563–573.

Boeckstaens, M., Andre, B., and Marini, A.M. (2008). Distinct transport mechanisms in yeast ammonium transport/sensor proteins of the mep/amt/rh family and impact on filamentation. J. Biol. Chem. *283*, 21362–21370.

Boeckstaens, M., Andre, B., and Marini, A.M. (2007). The yeast ammonium transport protein Mep2 and its positive regulator, the Npr1 kinase, play an important role in normal and

pseudohyphal growth on various nitrogen media through retrieval of excreted ammonium. Mol. Microbiol. *64*, 534–546.

Boeckstaens, M., Llinares, E., Van Vooren, P., and Marini, A.M. (2014). The TORC1 effector kinase Npr1 fine tunes the inherent activity of the Mep2 ammonium transport protein. Nat. Commun. *5*, 3101.

Boeckstaens, M., Merhi, A., Llinares, E., Van Vooren, P., Springael, J.-Y., Wintjens, R., and Marini, A.M. (2015). Identification of a novel regulatory mechanism of nutrient transport controlled by TORC1-Npr1-Amu1/Par32. PLoS Genet. *11*, e1005382.

Breitkreutz, a., Choi, H., Sharom, J.R., Boucher, L., Neduva, V., Larsen, B., Lin, Z.Y., Breitkreutz, B.J., Stark, C., Liu, G., et al. (2010). A global protein kinase and phosphatase interaction network in yeast. Science *328*, 1043–1046.

Courchesne, W.E., and Magasanik, B. (1983). Ammonia regulation of amino acid permeases in *Saccharomyces cerevisiae*. Mol. Cell Biol. *3*, 672–683.

Crespo, J.L., Helliwell, S.B., Wiederkehr, C., Demougin, P., Fowler, B., Primig, M., and Hall, M.N. (2004). NPR1 kinase and RSP5-BUL1/2 ubiquitin ligase control GLN3-dependent transcription in *Saccharomyces cerevisiae*. J. Biol. Chem. *279*, 37512–37517.

De Craene, J.O., Soetens, O., and Andre, B. (2001). The Npr1 kinase controls biosynthetic and endocytic sorting of the yeast Gap1 permease. J. Biol. Chem. *276*, 43939–43948.

De Virgilio, C., and Loewith, R. (2006). Cell growth control: little eukaryotes make big contributions. Oncogene *25*, 6392–6415.

Dechant, R., Saad, S., Ibáñez, A.J., and Peter, M. (2014). Cytosolic pH regulates cell growth through distinct GTPases, Arf1 and Gtr1, to promote Ras/PKA and TORC1 activity. Mol. Cell *55*, 409–421.

Di Como, C.J., and Arndt, K.T. (1996). Nutrients, via the Tor proteins, stimulate the association of Tap42 with type 2A phosphatases. Genes Dev. *10*, 1904–1916.

Dubois, E., and Grenson, M. (1979). Methylamine/ammonia uptake systems in *Saccharomyces cerevisiae*: multiplicity and regulation. Mol. Gen. Genet. *175*, 67–76.

Dubouloz, F., Deloche, O., Wanke, V., Cameroni, E., and De Virgilio, C. (2005). The TOR and EGO protein complexes orchestrate microautophagy in yeast. Mol. Cell *19*, 15–26.

Eltschinger, S., and Loewith, R. (2016). TOR complexes and the maintenance of cellular homeostasis. Trends Cell Biol. *26*, 148–159.

Fasolo, J., Sboner, A., Sun, M.G.F., Yu, H., Chen, R., Sharon, D., Kim, P.M., Gerstein, M., and Snyder, M. (2011). Diverse protein kinase interactions identified by protein microarrays reveal novel connections between cellular processes. Genes Dev. *25*, 767–778.

Feller, A., Boeckstaens, M., Marini, A.M., and Dubois, E. (2006). Transduction of the nitrogen signal activating Gln3-mediated transcription is independent of Npr1 kinase and Rsp5-Bul1/2 ubiquitin ligase in *Saccharomyces cerevisiae*. J. Biol. Chem. *281*, 28546–28554.

Fonseca, B.D., Diering, G.H., Bidinosti, M.A., Dalal, K., Alain, T., Balgi, A.D., Forestieri, R., Nodwell, M., Rajadurai, C.V., Gunaratnam, C., et al. (2012). Structure-activity analysis of niclosamide reveals potential role for cytoplasmic pH in control of mammalian target of rapamycin complex 1 (mTORC1) signaling. J. Biol. Chem. *287*, 17530–17545.

Gander, S., Bonenfant, D., Altermatt, P., Martin, D.E., Hauri, S., Moes, S., Hall, M.N., and Jenoe, P. (2008). Identification of the rapamycin-sensitive phosphorylation sites within the Ser/Thr-rich domain of the yeast Npr1 protein kinase. Rapid Commun. Mass Spectrom. *22*, 3743–3753.

Gnad, F., de Godoy, L.M.F., Cox, J., Neuhauser, N., Ren, S., Olsen, J.V., and Mann, M. (2009). High-accuracy identification and bioinformatic analysis of in vivo protein phosphorylation sites in yeast. Proteomics *9*, 4642–4652.

Godard, P., Urrestarazu, A., Vissers, S., Kontos, K., Bontempi, G., van, H.J., and Andre, B. (2007). Effect of 21 different nitrogen sources on global gene expression in the yeast *Saccharomyces cerevisiae*. Mol. Cell Biol. *27*, 3065–3086.

Gong, R., Li, L., Liu, Y., Wang, P., Yang, H., Wang, L., Cheng, J., Guan, K.-L., and Xu, Y. (2011). Crystal structure of the Gtr1p-Gtr2p complex reveals new insights into the amino acid-induced TORC1 activation. Genes Dev. *25*, 1668–1673.

González, A., and Hall, M.N. (2017). Nutrient sensing and TOR signaling in yeast and mammals. EMBO J. *36*, 397–408.

González, A., Ruiz, A., Casamayor, A., and Ariño, J. (2009). Normal function of the yeast TOR pathway requires the type 2C protein phosphatase Ptc1. Mol. Cell. Biol. *29*, 2876–2888.

González, A., Shimobayashi, M., Eisenberg, T., Merle, D.A., Pendl, T., Hall, M.N., and Moustafa, T. (2015). TORC1 promotes phosphorylation of ribosomal protein S6 via the AGC kinase Ypk3 in *Saccharomyces cerevisiae*. PLoS One *10*, e0120250.

Grenson, M. (1983a). Inactivation-reactivation process and repression of permease formation regulate several ammonia-sensitive permeases in the yeast *Saccharomyces cerevisiae*. Eur. J. Biochem. *133*, 135–139.

Grenson, M. (1983b). Study of the positive control of the general amino-acid permease and other ammonia-sensitive uptake systems by the product of the NPR1 gene in the yeast *Saccharomyces cerevisiae*. Eur. J. Biochem. *133*, 141–144.

Hatakeyama, R., Péli-Gulli, M.-P., Hu, Z., Jaquenoud, M., Garcia Osuna, G.M., Sardu, A., Dengjel, J., and De Virgilio, C. (2019). Spatially distinct pools of TORC1 balance protein homeostasis. Mol. Cell *73*, 325–338.e8.

Heitman, J., Movva, N.R., and Hall, M.N. (1991). Targets for cell cycle arrest by the immunosuppressant rapamycin in yeast. Science *253*, 905–909.

Holt, L.J., Tuch, B.B., Villen, J., Johnson, A.D., Gygi, S.P., and Morgan, D.O. (2009). Global analysis of Cdk1 substrate phosphorylation sites provides insights into evolution. Science *325*, 1682–1686.

Howell, J.J., Ricoult, S.J.H., Ben-Sahra, I., and Manning, B.D. (2013). A growing role for mTOR in promoting anabolic metabolism. Biochem. Soc. Trans. *41*, 906–912.

Huber, A., Bodenmiller, B., Uotila, A., Stahl, M., Wanka, S., Gerrits, B., Aebersold, R., and Loewith, R. (2009). Characterization of the rapamycin-sensitive phosphoproteome reveals that Sch9 is a central coordinator of protein synthesis. Genes Dev. *23*, 1929–1943.

Hughes Hallett, J.E., Luo, X., and Capaldi, A.P. (2015). Snf1/AMPK promotes the formation of Kog1/Raptor-bodies to increase the activation threshold of TORC1 in budding yeast. Elife *4*. https://doi.org/10.7554/eLife.09181.

Hughes Hallett, J.E., Luo, X., and Capaldi, A.P. (2014). State transitions in the TORC1 signaling pathway and information processing in *Saccharomyces cerevisiae*. Genetics *198*, 773–786.

Jacinto, E., Guo, B., Arndt, K.T., Schmelzle, T., and Hall, M.N. (2001). TIP41 interacts with TAP42 and negatively regulates the TOR signaling pathway. Mol. Cell *8*, 1017–1026.

Kawai, S., Urban, J., Piccolis, M., Panchaud, N., De Virgilio, C., and Loewith, R. (2011). Mitochondrial genomic dysfunction causes dephosphorylation of Sch9 in the yeast *Saccharomyces cerevisiae*. Eukaryot. Cell *10*, 1367–1369.

Kim, A., and Cunningham, K.W. (2015). A LAPF/phafin1-like protein regulates TORC1 and lysosomal membrane permeabilization in response to endoplasmic reticulum membrane stress. Mol. Biol. Cell *26*, 4631–4645.

Kira, S., Tabata, K., Shirahama-Noda, K., Nozoe, A., Yoshimori, T., and Noda, T. (2014). Reciprocal conversion of Gtr1 and Gtr2 nucleotide-binding states by Npr2-Npr3 inactivates TORC1 and induces autophagy. Autophagy *10*, 1565–1578.

Loewith, R., and Hall, M.N. (2011). Target of Rapamycin (TOR) in nutrient signaling and growth control. Genetics *189*, 1177–1201.

Loewith, R., Jacinto, E., Wullschleger, S., Lorberg, A., Crespo, J.L., Bonenfant, D., Oppliger, W., Jenoe, P., and Hall, M.N. (2002). Two TOR complexes, only one of which is rapamycin sensitive, have distinct roles in cell growth control. Mol. Cell *10*, 457–468.

MacDonald, C., and Piper, R.C. (2017). Genetic dissection of early endosomal recycling highlights a TORC1-independent role for Rag GTPases. J. Cell Biol. *216*, 3275–3290.

MacGurn, J.A., Hsu, P.-C., Smolka, M.B., and Emr, S.D. (2011). TORC1 regulates endocytosis via Npr1-mediated phosphoinhibition of a ubiquitin ligase adaptor. Cell *147*, 1104–1117.

Marini, A.M., Soussi-Boudekou, S., Vissers, S., and Andre, B. (1997). A family of ammonium transporters in *Saccharomyces cerevisiae*. Mol. Cell Biol. *17*, 4282–4293.

Merhi, A., and André, B. (2012). Internal amino acids promote Gap1 permease ubiquitylation via TORC1/Npr1/14-3-3-dependent control of the bul arrestin-like adaptors. Mol. Cell. Biol. *32*, 4510–4522.

Michaillat, L., Baars, T.L., and Mayer, A. (2012). Cell-free reconstitution of vacuole membrane fragmentation reveals regulation of vacuole size and number by TORC1. Mol. Biol. Cell *23*, 881–895.

Michel, A.H., Hatakeyama, R., Kimmig, P., Arter, M., Peter, M., Matos, J., De Virgilio, C., and Kornmann, B. (2017). Functional mapping of yeast genomes by saturated transposition. Elife *6*. https://doi.org/10.7554/eLife.23570.

Neklesa, T.K., and Davis, R.W. (2009). A genome-wide screen for regulators of TORC1 in response to amino acid starvation reveals a conserved Npr2/3 complex. PLoS Genet. *5*, e1000515.

Nicastro, R., Sardu, A., Panchaud, N., and De Virgilio, C. (2017). The architecture of the rag GTPase signaling network. Biomolecules *7*, 48.

Orij, R., Urbanus, M.L., Vizeacoumar, F.J., Giaever, G., Boone, C., Nislow, C., Brul, S., and Smits, G.J. (2012). Genome-wide analysis of intracellular pH reveals quantitative control of cell division rate by pHc in *Saccharomyces cerevisiae*. Genome Biol. *13*, R80.

Panchaud, N., Péli-Gulli, M.-P., and De Virgilio, C. (2013a). Amino acid deprivation inhibits TORC1 through a GTPase-activating protein complex for the rag family GTPase Gtr1. Sci. Signal. *6*, ra42.

Panchaud, N., Péli-Gulli, M.-P., and De Virgilio, C. (2013b). SEACing the gAP that nEGOCiates TORC1 activation. Cell Cycle *12*, 2948–2952.

Prouteau, M., Desfosses, A., Sieben, C., Bourgoint, C., Lydia Mozaffari, N., Demurtas, D., Mitra, A.K., Guichard, P., Manley, S., and Loewith, R. (2017). TORC1 organized in inhibited domains (TOROIDs) regulate TORC1 activity. Nature *550*, 265–269.

Rechsteiner, M., and Rogers, S.W. (1996). PEST sequences and regulation by proteolysis. Trends Biochem. *21*, 267–271.

Saliba, E., Evangelinos, M., Gournas, C., Corrillon, F., Georis, I., and Andre, B. (2018). The yeast H+-ATPase Pma1 promotes Rag/Gtr-dependent TORC1 activation in response to H+-coupled nutrient uptake. Elife *7*. https://doi.org/10.7554/eLife.31981.

Schmidt, A., Beck, T., Koller, A., Kunz, J., and Hall, M.N. (1998). The TOR nutrient signalling pathway phosphorylates NPR1 and inhibits turnover of the tryptophan permease. EMBO J. *17*, 6924–6931.

Shimobayashi, M., and Hall, M.N. (2014). Making new contacts: the mTOR network in metabolism and signalling crosstalk. Nat. Rev. Mol. Cell Biol. *15*, 155–162.

Stracka, D., Jozefczuk, S., Rudroff, F., Sauer, U., and Hall, M.N. (2014). Nitrogen source activates TOR (target of rapamycin) complex 1 via glutamine and independently of Gtr/Rag proteins. J. Biol. Chem. *289*, 25010–25020.

Tanigawa, M., and Maeda, T. (2017). An in vitroTORC1 kinase assay that recapitulates the Gtr-independent glutamine-responsive TORC1 activation mechanism on yeast vacuoles. Mol. Cell. Biol. *37*, e00075–17.

Ukai, H., Araki, Y., Kira, S., Oikawa, Y., May, A.I., and Noda, T. (2018). Gtr/Ego-independent TORC1 activation is achieved through a glutamine-sensitive interaction with Pib2 on the vacuolar membrane. PLoS Genet. *14*, e1007334.

Urban, J., Soulard, A., Huber, A., Lippman, S., Mukhopadhyay, D., Deloche, O., Wanke, V., Anrather, D., Ammerer, G., Riezman, H., et al. (2007). Sch9 is a major target of TORC1 in *Saccharomyces cerevisiae*. Mol. Cell *26*, 663–674.

Vandenbol, M., Jauniaux, J.C., and Grenson, M. (1990). The *Saccharomyces cerevisiae* NPR1 gene required for the activity of ammonia-sensitive amino acid permeases encodes a protein kinase homologue. Mol.Gen.Genet. *222*, 393–399.

Varlakhanova, N.V., Tornabene, B.A., and Ford, M.G.J. (2018). Feedback regulation of TORC1 by its downstream effectors Npr1 and Par32. Mol. Biol. Cell *29*, 2751–2765.

Varlakhanova, N.V., Mihalevic, M.J., Bernstein, K.A., and Ford, M.G.J. (2017). Pib2 and the EGO complex are both required for activation of TORC1. J. Cell Sci. *130*, 3878–3890.

Wullschleger, S., Loewith, R., and Hall, M.N. (2006). TOR signaling in growth and metabolism. Cell *124*, 471–484.

Yuan, W., Guo, S., Gao, J., Zhong, M., Yan, G., Wu, W., Chao, Y., and Jiang, Y. (2017). General control nonderepressible 2 (GCN2) kinase inhibits target of rapamycin complex 1 in response to amino acid starvation in *Saccharomyces cerevisiae*. J. Biol. Chem. *292*, 2660–2669.

Zoncu, R., Bar-Peled, L., Efeyan, A., Wang, S., Sancak, Y., and Sabatini, D.M. (2011). mTORC1 senses lysosomal amino acids through an inside-out mechanism that requires the vacuolar H+-ATPase. Science *334*, 678–683.

**ISCI, Volume *20***

## Supplemental Information

# Pib2-Dependent Feedback Control of the TORC1 Signaling Network by the Npr1 Kinase

**Ana Sofia Brito, Silvia Soto Diaz, Pascale Van Vooren, Patrice Godard, Anna Maria Marini, and Mélanie Boeckstaens**

**Figure S1, related to Figure 2A and 2E.** Immunodetection of GFP-Npr1 from total extracts of cells grown in the presence of proline as a nitrogen source. Pgk1 was detected as a loading control. Wild-type (23344c), *gtr1Δ gtr2Δ* (MB386) and *snf1Δ* (PVV334) cells were transformed with p*MET25*-GFP-Npr1.

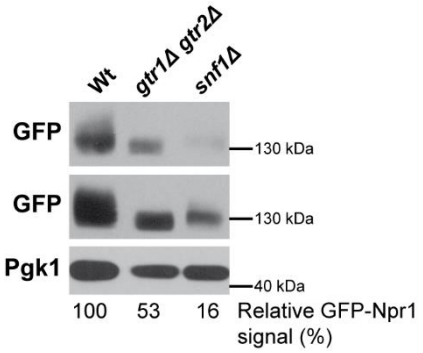

**Figure S2, related to Figure 2E and 2I.** (A) Quantification of Npr1 abundance after glutamine addition from the data shown in Figure 2I (Wt, *pib2Δ*) and 2E (*gtr1Δ gtr2Δ*) and normalized using the control Pgk1 signal. (B) Immunodetection of HA-Npr1 from total extracts of wild-type (23344c) and *pib2Δ* (PVV329) cells transformed with pAS103. At time 0, glutamine (0.1%) was added to the cell culture grown in the presence of proline as nitrogen source. Pgk1 was detected as a loading control. (C) Quantification of Npr1 abundance from the data shown in Figure S2B and normalized using the control Pgk1 signal.

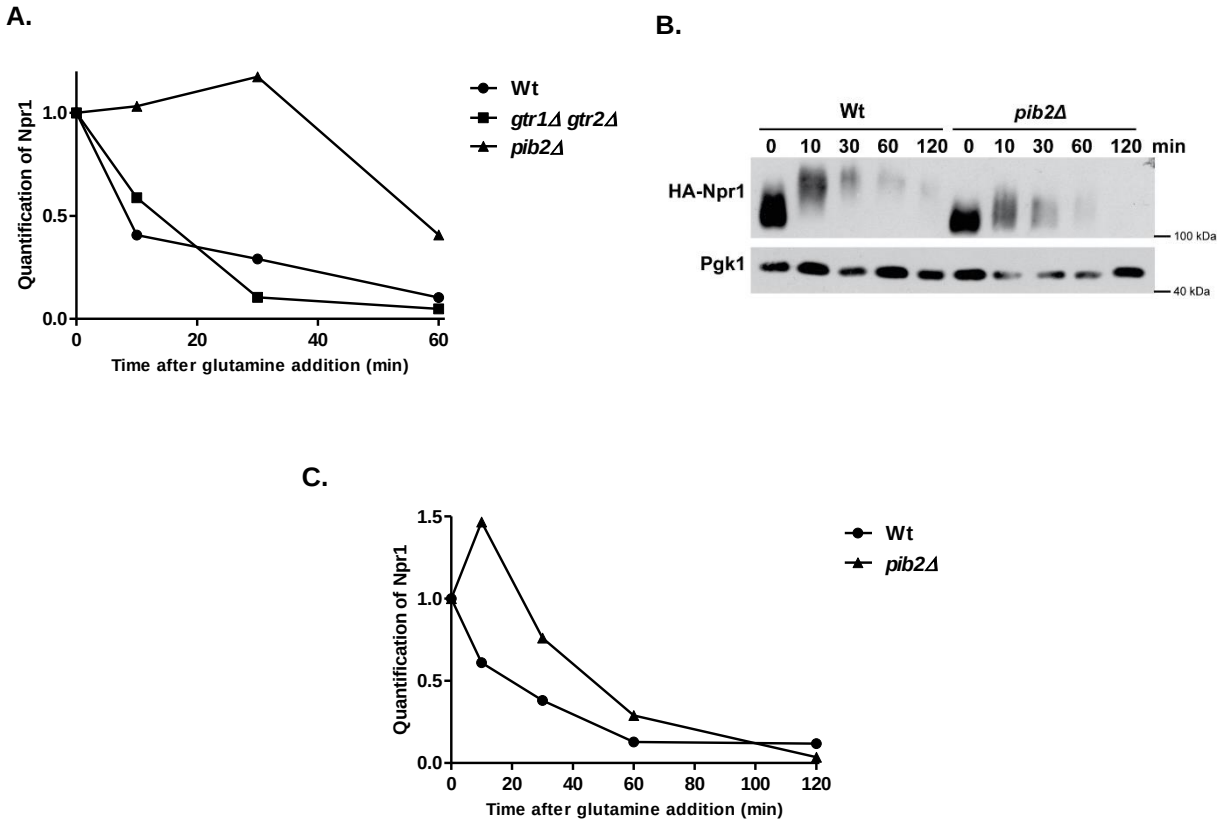

**Figure S3, related to Figure 5A.** (A) Immunodetection of GFP-Npr1 from total extracts. *npr1Δ* (PVV357) cells were transformed with p*MET25*-GFP-Npr1, p*MET25*-GFP-Npr1$^{414Start}$, p*MET25*-GFP-Npr1$^{438Start}$, and p*MET25*-GFP-Npr1$^{K467R}$, and grown in the presence of proline as nitrogen source. Pgk1 was detected as a loading control.

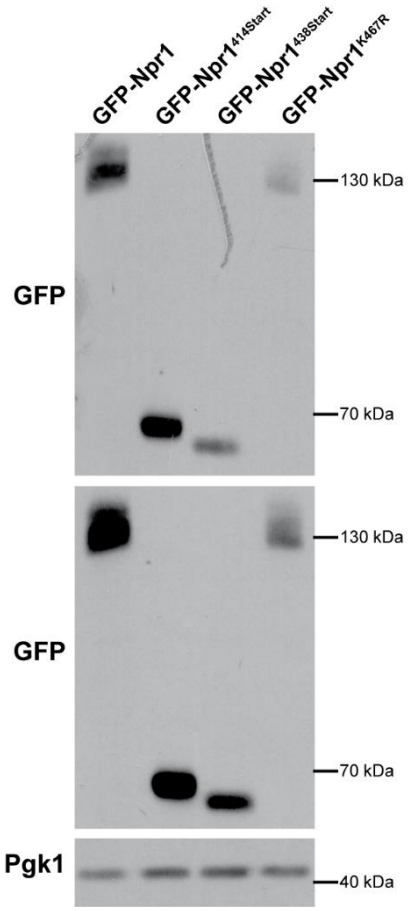

**Table S1.** List of yeast strains used in this study.

| Strain | Genotype | Source or reference |
|---|---|---|
| 23344c | *ura3* | Lab collection |
| 30788a | *npr1Δ ura3* | (De Craene et al., 2001) |
| 31019b | *mep1Δ mep2Δ::LEU2 mep3Δ::KanMX2 ura3* | (Marini et al., 1997) |
| 36307b | *AMU1-HA npr1Δ ura3* | (Boeckstaens et al., 2015) |
| MB142 | *AMU1-HA ura3* | (Boeckstaens et al., 2015) |
| MB383 | *gcn2Δ ura3* | This study |
| MB386 | *gtr1Δ gtr2Δ ura3* | This study |
| MB393 | *VPH1-mCherry ura3* | This study |
| PVV318 | *gtr1Δ ura3* | This study |
| PVV329 | *pib2Δ ura3* | This study |
| PVV334 | *snf1Δ ura3* | This study |
| PVV353 | *VPH1-mCherry npr1Δ ura3* | This study |
| PVV357 | *npr1Δ ura3* | This study |
| PVV363 | *pib2Δ npr1Δ ura3* | This study |
| PVV366 | *gtr1Δ gtr2Δ npr1Δ ura3* | This study |

**Table S2.** List of plasmids used in this study.

| Plasmid | Description | Source or reference |
|---|---|---|
| **Low-copy-number** | | |
| pFL38 | YCpFL38 (*CEN-ARS URA3*) | (Bonneaud et al., 1991) |
| YCpNpr1 | YCpFL38 *promNPR1*- NPR1 | This study |
| YCpNpr1$^{K467R}$ | YCpFL38 *promNPR1*- NPR1$^{K467R}$ | This study |
| YCpAmu1-3HA | YCpFL38 AMU1-3HA | (Boeckstaens et al., 2015) |
| YCpGFP-Pib2 | p416*MET25- yEGFP3-PIB2* | This study |
| YCpGFP-Npr1 | p416*MET25-yEGFP3-NPR1* | This study |
| YCpGFP-Npr1$^{414Start}$ | p416*MET25- yEGFP3-NPR1$^{414Start}$* | This study |
| YCpGFP-Npr1$^{438Start}$ | p416*MET25- yEGFP3-NPR1$^{438Start}$* | This study |
| YCpGFP-Npr1$^{K467R}$ | p416*MET25-yEGFP3-NPR1$^{K467R}$* | This study |
| pUG36 | p416*MET25-yEGFP3, URA3* | Gift from J.H. Hegemann |
| **High-copy-number** | | |
| pFL44 | YEpFL44 (*2µ URA3*) | (Bonneaud et al., 1991) |
| pAS103 | YEplac195 *HA-NPR1* | (Schmidt et al., 1998) |
| pYES-pHluorin | pYES-pHluorin | (Orij et al., 2009) |
| YEpNpr1 | YEpFL44 *promNPR1*- NPR1 | This study |
| YEpNpr1$^{K467R}$ | YEpFL44 *promNPR1*- NPR1$^{K467R}$ | This study |
| YEpHA-Npr1 | YEpFL44 *promNPR1*- HA-NPR1 | This study |

## Transparent Methods

*Strains, growth conditions*

The *S. cerevisiae* strains used in this study are listed in Table S1. All strains are isogenic with the wild type Σ1278b (Bechet et al., 1970). Cell transformation and gene deletions were performed as described previously (Gietz et al., 1992; Wach et al., 1994). Cells were grown in a rich-medium or in a buffered (pH 6.1) minimal medium with 3% glucose as the carbon source (Jacobs et al., 1980). To this medium, nitrogen sources were added as required by the experiment and as specified in the text. The nitrogen sources used were 0.1% proline, 0.1% citrulline, 0.1% valine, glutamine, 0.1% glutamate, or $(NH_4)_2SO_4$ at the specified concentration. For rapamycin recovery, cells were exposed to rapamycin (160 ng/ml) or to the rapamycin vehicle alone (ethanol/tween) for 3h. Cells were then washed two times and plated on rich medium or on a minimal medium containing glutamine 0.1% as nitrogen source. Cells were imaged after 2 days of growth.

*Plasmids*

Plasmids used in this study are listed in Table S2. Primers used in this study are available upon request. YCpGFP-Pib2, YCpGFP-Npr1, YCpGFP-Npr1$^{414Start}$, YCpGFP-Npr1$^{438Start}$: the *PIB2* and *NPR1* genes, as well as the truncated forms of *NPR1*, were amplified by PCR from the genomic DNA from *S. cerevisiae* wild-type strain (23344c) and cloned in the HindIII and XhoI restriction sites of the pUG36 vector, kindly provided by J.H. Hegemann. YCpNpr1, YEpNpr1: the *NPR1* gene and a promoter region encompassing 500 pb was amplified by PCR from the genomic DNA from *S. cerevisiae* wild-type strain (23344c) and cloned in the SalI and XbaI restriction sites of the of the pFL38 or pFL44 vectors (Bonneaud et al., 1991). YEpHA-Npr1: A PCR fragment comprising a part of the HA-tagged *NPR1* gene (40 pb) and its promoter region (40 pb upstream the SpeI restriction site) was amplified from pAS103. A PCR fragment comprising a part of the *NPR1* gene (between the START codon and after the SpeI restriction site) was amplified from YCpNpr1. These two amplifications were used to replace by *in vivo* recombination *NPR1* gene by *HA-NPR1* gene in the plasmid YEpNpr1 (digested by SpeI). All constructs were verified by sequencing (Genewiz). YCpGFP-Npr1$^{K467R}$, YCpNpr1$^{K467R}$ and YEpNpr1$^{K467R}$: were obtained by site-directed mutagenesis of *NPR1* performed using the Quick Change Site-directed Mutagenesis Kit (Stratagene).

*In vivo pH measurement*

Cells were transformed with the plasmid enabling cytosolic pHluorin expression, pYES-pHluorin (Orij et al., 2009). For the calibration curve, about $10^7$ exponentially growing cells were centrifuged for 5 min at 14,000 rpm and resuspended in PBS containing 100 µg/ml digitonine. After 15 min of gentle agitation (rotating wheel), cells were centrifuged and resuspended in $Na_2HPO_4$/citrate buffer of pH values ranging from 4.8 to 8.1. Fluorescence emission at 510 nm was measured at two excitation wavelengths (395 and 475 nm) using an Infinite M200pro (Tecan) microplate reader. For each pH value, the ratio of fluorescence intensity values (F395/F475) was calculated and data of two strains (Wt, *npr1*) from 6 independent experiments were pooled. Pooled ratio values were plotted with a fitted nonlinear curve, corresponding to the calibration curve. To measure *in vivo* cytosolic pH, cells expressing pHluorin were grown to the exponential phase and 200µl of culture containing about $0.2x10^7$ cells were used. Fluorescence emitted at 510 nm was directly measured at two excitation wavelengths (395 and 475 nm), and the ratio of fluorescence intensity values (F395/F475) was calculated. The pH values were calculated by extrapolating the ratio values on the calibration curve. When relevant, evolution of $pH_c$ corrected for negative control variations (delta-pH) was calculated by subtracting for each time point the average of pH values of the negative control from pH values of interest conditions.

*Western immunoblotting*

Total protein extracts were performed as described previously (Volland et al., 1994). Membrane-enriched cell extracts were prepared as described previously (Boeckstaens et al., 2007). For blot analysis, equal protein amounts (~20 µg) were loaded onto an 6% to 10% SDS-polyacrylamide gel in a Tricine system (Schagger and von Jagow, 1987). After transfer to a nitrocellulose membrane (Protran, VWR), proteins were probed with a mouse or rabbit antiserum raised against the C-terminal region of Mep2 (1:2000) (Marini and Andre, 2000), a peptide (PEPIRpSKTSAQM) centred on phosphoS457 of Mep2 (Genecust) (Boeckstaens et al., 2014), Gap1 (1:10000) (De Craene et al., 2001), Pgk1 (1:10000) (Invitrogen), total Rps6 (1:4000) (Bethyl), pRps6 (pS235-236) (1:2000) (#4858, Cell Signaling Technology), HA (1:10000) (Roche), GFP (1:10000) (Roche) and Pma1 (1:10000) (De Craene et al., 2001). Primary antibodies were detected with horseradish-peroxidase-conjugated anti-rabbit- or anti-mouse-IgG secondary antibodies (GE Healthcare) followed by measurement of chemoluminescence

(Lumi-Light$^{PLUS}$, Roche). For alkaline phosphatase treatment on total cell lysates, the protein pellet collected after TCA precipitation was resuspended in a solution (0.1 M Tris-HCl pH 6.8, 20% glycerol, 4% SDS, 2% β-mercaptoethanol and 2 mM PMSF) containing proteases inhibitors (Complete Mini, Roche). This lysate was diluted 5 X in a dephosphorylation buffer [CIP 1X (Roche), 50 mM Tris-HCl 1M pH 6.8, 2 mM PMSF] containing proteases inhibitors (Complete Mini, Roche). pH was eventually adjusted to 7.6 and extracts were incubated 1h at 37°C in the presence (or absence) of 10 units of calf alkaline phosphatase (Roche). Proteins were precipitated with 10% TCA. For PNGase F treatment on membrane-enriched cell extracts, the collected membrane pellet was suspended in buffer (1X PBS, 10 mM EDTA pH8, 0.5 % octyl glucopyranoside, 0.2 % 2-mercaptoethanol, 3 mM PMSF and proteinase inhibitors) and incubated 1h at 37°C in the presence (or absence) of 1.5 unit of peptide-N-glycosidase F (PNGase F, Sigma-Aldrich, Roche). Proteins were precipitated with 10% TCA.

*Fluorescence microscopy*

Images were acquired using a Zeiss LSM710 laser-scanning confocal microscope, equipped with the Airy scan module. Acquisitions were performed using the ZEN 2.1 software and images were processed using ImageJ (Schneider et al., 2012). The acquisition parameters were the same for all the conditions: scan speed 7 (scan time: 10.89 s), pinhole 3.14 airy units (0.4 µm section). The significance of the differences of proportions of cells containing GFP-Pib2 puncta in the different conditions has been assessed by a Wilcoxon two-sided rank test. The same approach has been applied for assessing the significance of the differences of proportions of cells with a fragmented vacuole. Cells were considered as containing fragmented vacuoles if more than 4 vacuolar lobes were observed.

**SUPPLEMENTAL REFERENCES**


Bechet, J., Grenson, M., Wiame, J.M., 1970. Mutations affecting the repressibility of arginine biosynthetic enzymes in Saccharomyces cerevisiae. Eur.J.Biochem. 12, 31–39.

Boeckstaens, M., Andre, B., Marini, A.M., 2007. The yeast ammonium transport protein Mep2 and its positive regulator, the Npr1 kinase, play an important role in normal and pseudohyphal growth on various nitrogen media through retrieval of excreted ammonium. Mol Microbiol. 64, 534–546.

Boeckstaens, M., Llinares, E., Van Vooren, P., Marini, A.M., 2014. The TORC1 effector kinase Npr1 fine tunes the inherent activity of the Mep2 ammonium transport protein. Nat. Commun. 5, 3101. https://doi.org/10.1038/ncomms4101

Boeckstaens, M., Merhi, A., Llinares, E., Van Vooren, P., Springael, J.-Y., Wintjens, R., Marini, A.M., 2015. Identification of a Novel Regulatory Mechanism of Nutrient Transport Controlled by TORC1-Npr1-Amu1/Par32. PLoS Genet. 11, e1005382. https://doi.org/10.1371/journal.pgen.1005382

Bonneaud, N., Ozier-Kalogeropoulos, O., Li, G.Y., Labouesse, M., Minvielle-Sebastia, L., Lacroute, F., 1991. A family of low and high copy replicative, integrative and single-stranded S. cerevisiae/E. coli shuttle vectors. Yeast 7, 609–615.

De Craene, J.O., Soetens, O., Andre, B., 2001. The Npr1 kinase controls biosynthetic and endocytic sorting of the yeast Gap1 permease. J Biol Chem. 276, 43939–43948.

Gietz, D., St, J.A., Woods, R.A., Schiestl, R.H., 1992. Improved method for high efficiency transformation of intact yeast cells. Nucleic Acids Res. 20, 1425.

Jacobs, P., Jauniaux, J.C., Grenson, M., 1980. A cis-dominant regulatory mutation linked to the argB-argC gene cluster in Saccharomyces cerevisiae. J.Mol.Biol. 139, 691–704.

Marini, A.M., Andre, B., 2000. In vivo N-glycosylation of the mep2 high-affinity ammonium transporter of Saccharomyces cerevisiae reveals an extracytosolic N-terminus. Mol.Microbiol. 38, 552–564.

Marini, A.M., Soussi-Boudekou, S., Vissers, S., Andre, B., 1997. A family of ammonium transporters in Saccharomyces cerevisiae. Mol.Cell Biol. 17, 4282–4293.

Orij, R., Postmus, J., Ter Beek, A., Brul, S., Smits, G.J., 2009. In vivo measurement of cytosolic and mitochondrial pH using a pH-sensitive GFP derivative in Saccharomyces cerevisiae reveals a relation between intracellular pH and growth. Microbiology 155, 268–78. https://doi.org/10.1099/mic.0.022038-0

Schagger, H., von Jagow, G., 1987. Tricine-sodium dodecyl sulfate-polyacrylamide gel electrophoresis for the separation of proteins in the range from 1 to 100 kDa. Anal.Biochem. 166, 368–379.

Schmidt, A., Beck, T., Koller, A., Kunz, J., Hall, M.N., 1998. The TOR nutrient signalling pathway phosphorylates NPR1 and inhibits turnover of the tryptophan permease. EMBO J 17, 6924–6931.

Schneider, C.A., Rasband, W.S., Eliceiri, K.W., 2012. NIH Image to ImageJ: 25 years of image analysis. Nat. Methods 9, 671–5.

Volland, C., Urban-Grimal, D., Geraud, G., Haguenauer-Tsapis, R., Géraud, G., Haguenauer-Tsapis, R., 1994. Endocytosis and degradation of the yeast uracil permease under adverse conditions. J Biol Chem. 269, 9833–41.

Wach, A., Brachat, A., Pohlmann, R., Philippsen, P., 1994. New heterologous modules for classical or PCR-based gene disruptions in Saccharomyces cerevisiae. Yeast 10, 1793–1808.